An optimization framework for the network design of advanced district thermal energy systems

Amy Allen[a,b,*], Gregor Henze[a,b,c], Kyri Baker[a,b,c], Gregory Pavlak[d], Michael Murphy[e]

[a] *Department of Civil, Environmental and Architectural Engineering, University of Colorado Boulder, UCB 428, Boulder, 80309, Colorado, United States*
[b] *National Renewable Energy Laboratory, 15013 Denver West Parkway, Golden, 80401, Colorado, United States*
[c] *Renewable and Sustainable Energy Institute, 027 UCB, Boulder, 80309, Colorado, United States*
[d] *Department of Architectural Engineering, Pennsylvania State University, 104 Engineering Unit A, University Park, 16802, Pennsylvania, United States*
[e] *Department of Process, Energy and Transport Engineering, Munster Technological University, Bishopstown, Cork, Ireland*

Abstract

In this work, a topology optimization framework for district thermal energy systems is presented. The framework seeks to to address the questions, for a given district, "What is the best subset of buildings to connect to a district thermal energy system, and by what network should they be connected, to minimize life cycle cost?" A particle swarm optimization approach is validated to address the selection of the subset of buildings, and a graph theory-based heuristic is validated for selection of the network topology for any candidate subset of buildings. The framework is applied to a prototypical urban district for illustrative purposes. Modeling of prototypical districts

---

[*] Corresponding author

Email address: `amy.allen@colorado.edu` (Amy Allen)

Preprint submitted to Energy Conversion and Management *May 27, 2022*

revealed reductions in source energy use intensity for heating and cooling of 21-25% through the use of advanced district energy systems relative to code-compliant, building level systems. The framework identifies solutions with life cycle cost values 14% to 72% lower than that of base case scenarios based on conventional design approaches, depending on the base case scenario selected. Analysis of the search space indicates that topology optimization facilitates reductions in life cycle cost, source energy use intensity, and carbon emissions.

Keywords: District thermal energy systems, ambient loops, topology optimization, particle swarm optimization

PACS: 0000, 1111

2000 MSC: 0000, 1111

---

1. Introduction

A scientific consensus has emerged that widespread electrification of space heating will be necessary to meet targets for deep decarbonization in the U.S. while minimizing the need for costly technologies to capture and sequester carbon emissions [1]. The U.S. National Academies of Science, Engineering, and Medicine recently called for electrification of heating in new construction in much of the United States by 2030, in order for the country to reach net-zero carbon emissions by 2050, and avert the worst consequences of climate change [2]. The European Commission concluded that averting global temperature rise of more than 1.5 °C by 2100 would likely require electrification of more than 60% of energy end uses in buildings by 2050, and that a similar degree of electrification would be required in buildings in China in order to avert global temperature rise of more than 2 °C. [3] . Given worldwide trends towards urbanization, it is expected that 68% of people will be living in cities by 2050 [4]. District thermal energy systems (DES) operating at near-ambient temperatures facilitate beneficial electrification of heating in urban districts, as well as significant reductions in source-energy use intensity (EUI) in appropriate applications. However, such systems face barriers to adoption, especially in the United States, due to their high infrastructure costs, and the very large search space of potential network configurations, which complicates their design.

In this paper, a novel framework for network topology optimization of DES is presented, and the techniques that it leverages –a graph theory-based heuristic and an optimization approach– are validated. The framework is then applied to a prototypical district as a case study, to quantify the potential benefits of the approach. The Topology Optimization Framework ("framework") is particularly relevant in the context of emerging DES operating at near-ambient temperatures, but the general approach is extensible to other types of DES as well.

1.1. Fifth-generation district heating and cooling systems

This work will adopt the definition of fifth-generation district heating and cooling (5GDHC) systems proposed by [5]. Such systems are distinguished from earlier generations of DES through their use of water at near-ambient temperatures (15 °C - 25 °C) as a working fluid, and the use of water-source heat pumps at connected buildings, which operate with the network as a heat source and sink [5]. The near-ambient water temperatures used by 5GDHC systems are conducive to the integration of lower-temperature waste heat sources, as well as renewable thermal sources, and facilitate the use of electrically-driven heat pumps, and thus, the decarbonization of source energy for heating [6]. The more moderate operating temperatures of 5GDHC systems also creates the potential for connected loads to act as *prosumers*, and exchange heat (or heat rejection) in a synergistic manner [7]. This motivates the consideration of meshed thermal network configurations, beyond the radial or ring networks that are commonly used in earlier generations of DES, and makes the question of network topology optimization especially relevant.

1.2. Relevant concepts from graph theory

In this work, thermal networks will be described using concepts from graph theory. In mathematics, a graph is defined as a set of nodes (vertices) and edges (pairs of vertices) [8]. In the context of a thermal network, nodes represent connected loads and centralized supply equipment, and edges represent thermal connections (pipes carrying the working fluid). A graph can be represented with an adjacency matrix, a square matrix with dimension equal to the number of nodes. A given element of the adjacency matrix has the value of unity if there exists a connection between the corresponding nodes, and a value of zero otherwise. Of particular interest in the context of thermal networks are *connected graphs*, in which there exists at least one path between each pair of nodes. A *spanning tree* is a type of connected graph in which there exists *exactly* one path between each pair of nodes. A *minimal spanning tree* (MST) is the spanning tree that connects the given nodes with the least total edge length [8]. In the context of a thermal network, the MST minimizes the total network length, and thus, the infrastructure cost. In general, the infrastructure cost is often a significant fraction of the overall life cycle cost (LCC) of a district thermal energy system [9].

1.3. Particle swarm optimization

The network topology optimization problem as defined here is non-convex. Non-convex optimization problems motivate the use of so-called metaheuristic techniques, which, while not offering a guarantee of convergence at the global optimum, are often effective at finding near-optimal solutions, in an efficient manner (relative to an exhaustive search) [10]. Metaheuristics do not require an explicit definition of the objective function or its gradient, making them compatible with the use of a "black box" function evaluator. Particle swarm optimization (PSO) is one such metaheuristic approach. Like other metaheuristics, PSO mimics a search process. Past work has suggested that relative to other metaheuristics, PSO has a lower risk of getting "stuck" at a local minimum [11]. PSO has been implemented in other problems in the building energy use domain, including by [12] and [13]. In the PSO context, "particles" can be interpreted as animals acting as part of a swarm in the natural world, seeking a location that maximizes the value of a certain objective [14]. Particles retain knowledge of both their own prior best location, and that of the best location visited by any member of the group, and are attracted back to both of these locations, to varying extents. For application to the network topology optimization problem for DES, the implementation of PSO for problems with discrete, binary variables is of interest. The work of [15] developed such an approach.

1.4. Topology optimization of district thermal energy systems

There is an extensive body of work in the area of optimization of different aspects of DES, including network topology and operating parameters, across different system generations. Past studies can be distinguished based on the type of cost function considered, as well as the generation of system, which has implications for the optimization variables. The work of [9] addressed a network topology optimization problem to minimize a LCC metric for a district heating system operating at 55 °C. The LCC metric considered encompassed infrastructure (pipes and distribution pumps), energy associated with pumping and heat losses, and a carbon tax. The optimization variables included pipe diameters (with a zero diameter corresponding to the non-existence of a thermal connection) and the location of a central heating plant. The authors formulated the problem as a mixed-integer nonlinear programming problem (MINLP), and employed genetic algorithms to solve it. Only tree network topologies were considered, and the connected building loads were taken as a boundary condition.

The work of [16] addressed a network topology optimization problem for a third-generation DES, to minimize the value of a LCC metric based on costs for piping and trenching, and a limited set of operating costs. The authors compared the optimal network configuration they determined to the network with minimal first cost, and found limited benefits in LCC, though a more significant savings in terms of the internal rate of return. The authors of [16] treated the connected loads as a boundary condition, and also treated the energy consumption of centralized equipment as static. They identified addressing the selection of loads to connect to a DES as an area in which further work was needed.

Other past studies have taken a multi-objective approach to optimization of DES. The work of [17] solved an optimization problem for the network topology and selection of primary equipment for a district heating network, to minimize LCC and carbon emissions, using an ϵ-constrained approach. The authors of [17] compared the optimally-designed district heating network to a scenario in which buildings were served by independent heating systems, and found a 23% reduction in carbon emissions, for the same initial investment.

The work of [18] applied adjoint-based methods to an optimization problem for a district heating system, with the optimization variables including the network topology and pipe diameters, as well as valve positions at connected loads, and the rate of heat supplied by individual pieces of centralized equipment. The authors considered an objective function based on the investment cost of piping and distribution pumps, and the operating cost for pumping. They developed an approach to project a continuous-valued diameter variable onto a set of discrete values of available pipe diameters, using a modified version of the *projection method* often used in structural topology optimization, and structured the cost function to penalize intermediate values of this variable. The use of adjoint-based methods, in conjunction with constraint aggregation, facilitated a large-scale analysis, considering a network with 160 connected loads. Through their topology optimization approach, they identified a network with a 23% reduction in piping cost relative to a base case. The connectivity status of the loads was taken as a boundary condition.

The authors of [19] optimized topology configuration, pipe diameter, and the values of other operating parameters (including supply and return temperatures and mass flow rates) for a district heating system to minimize LCC. The LCC metric considered included costs for infrastructure (primary plant equipment and piping and trenching) and energy use (for heat generation and circulation pumps). Their study considered both parallel and series connection of loads to the network, as well as the connection status of an individual building. Series connections were of interest in the context of buildings with lower temperature supply requirements. The authors of [19] divided the problem into three sub-problems: a MINLP, a mixed integer linear program, and a non-linear program. The authors considered steady-state conditions only. They applied their approach to several configurations of building locations and loads, and determined that solutions to the topology optimization problem were not generalizable.

1.5. Contribution

The work of [16] identified a need for work in topology optimization for DES to address both the selection of buildings to connect to a district thermal energy system, as well as the network by which they should be connected. Additionally, past work in the area of network topology optimization for DES, such as that of [19] and [20], has focused on model formulations oriented around specific case studies. Many past studies, such as those of [9] and [16], have not addressed the full scope of building energy use for heating, ventilation, and air-conditioning (HVAC). To the authors' knowledge, existing studies have not applied a comprehensive network topology optimization approach to DES operating at near-ambient temperatures, in the context of which the problem is particularly interesting and relevant. The presented framework seeks to address the question, for a given urban district, with known building locations and loads, “What is the best subset (if any) of buildings to connect to a district thermal energy system (DES), and by what network should they be connected, to minimize LCC?” It was hypothesized that a PSO algorithm could effectively identify the optimal subset of buildings, addressing the first part of the problem, and that the MST heuristic could effectively select the optimal thermal network by which to connect them, addressing the second.

The framework is novel because it addresses both the selection of loads to connect to a DES, as well as the network by which they should be connected, and addresses investment and operating costs in a comprehensive way, accounting for all HVAC-related energy consumption by a considered district. The compatibility with a user-supplied underlying energy model of high fidelity makes it highly extensible and suitable for detailed analysis of potential trade-offs. This contribution is also distinct from past work in that the framework has been evaluated in case studies involving 5GDHC systems with bi-directional thermal and mass flow. The development of the Topology Optimization Framework builds on the work of [21] in modeling and automated analysis of 5GDHC systems and extends previous work by the authors to evaluate the MST heuristic [22]. In this work, the development of the framework itself and its application in a case study are presented for the first time. While a particular DES model is employed for illustrative purposes in this study, the framework is generally extensible to any system model meeting certain conditions, discussed in more detail in Section 4.

In the following sections of this paper, the methods for validating the heuristic and optimization approach are discussed, results from the validation and application of the framework are presented, the structure of the developed framework is discussed, and conclusions about the potential of 5GDHC systems are presented.

2. Methods

The following subsections describe the formulation of the optimization problem, how these approaches were validated, and the application of the framework to a case study to quantify the benefits of the approach. The workflow of the Topology Optimization Framework is outlined schematically in Figure 1.

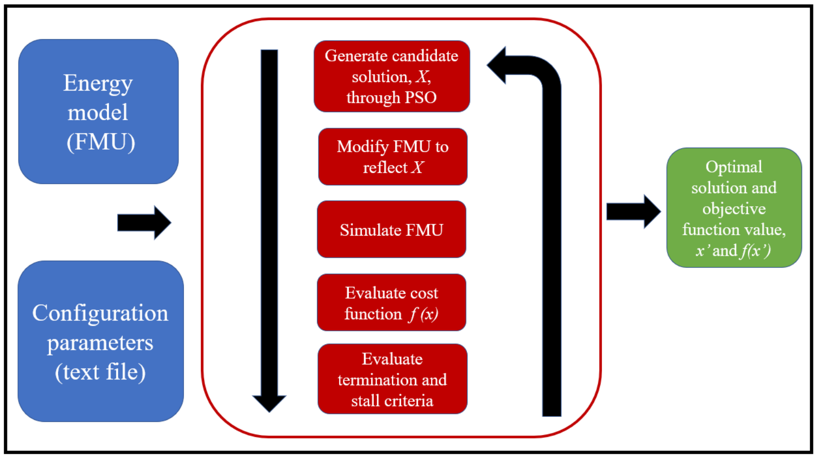

Figure 1: Diagram illustrating the workflow of the presented Topology Optimization Framework

2.1. Optimization problem

The cost function considered in the network topology optimization problem represents the LCC associated with meeting the heating and cooling loads of all buildings in the prototypical district, whether they are served by independent systems or the DES. The LCC considered includes energy costs for HVAC, costs associated with a potential future price on carbon, and infrastructure costs for the thermal network of the DES, evaluated over a thirty-year time period.[1] The LCC is calculated as shown in Eqn. 1:

$$\begin{aligned}&\min_{\vec{L}} C_{pipes} + C_{elec}UPV_{elec}(E_{de} + \sum_{i=1}^{n} E_{be,i}) + C_{gas}UPV_{gas}\sum_{j=1}^{n} E_{bg,j}\\&+ UPV_{CO2}\sum_{t=1}^{30} m_{CO2}(t)C_{CO2}(t)\end{aligned} \tag{1}$$

subject to:

(1) For $i, j \in \{1 \ldots n+1\}$, such that $j > i, A_{i,j} = L_{i+j-1}$

(2) If there exists a pipe directly thermally connecting building i and building j, $A_{i,j} = 1$. Otherwise, $A_{i,j} = 0$.

(3) If building i is served by the DES, there exists a path from the central plant to node i.

(4) $\forall i, j \in \{1 \ldots n+1\}, A_{i,j} = A_{j,i}$.

Note that since, in the context of this application, all thermal connections are treated as bi-directional, the adjacency matrix **A** must be symmetrical, and it can thus be represented with its upper-triangular elements only. Constraints 1, 2, and 4 address the construction of the adjacency matrix. Constraint 3 is a definition – a building is considered to be served by the DES if

---

[1] It was assumed that differential costs between the centralized and distributed heat pumps associated with the DES and building-level primary equipment would be small relative to the overall LCC. This could be refined in future work.

and only if a path exists between it and the centralized heat pump through a thermal network. The total number of network nodes is equal to $n + 1$, corresponding to all buildings considered and the centralized heat pump.

The uniform present value (UPV) factors are used to convert a cost incurred in one year to a cost over 30 years, accounting for the time value of money. The UPV factors applied for natural gas and electricity account for projected escalation in the costs of those commodities. The cost function was originally adapted from that used by [21]. Note that the optimization problem as formulated in Eqn. 1 is non-convex, due to the binary optimization variables, and the nature of the function through which HVAC energy consumption is calculated. Table 1 shows a summary of values of parameters used in the LCC calculation.

2.2. Prototypical districts

An exhaustive search, considering all potential thermal network configurations, was performed for a prototypical urban district in order to evaluate the performance of the MST heuristic and the implementation of PSO. As a case study, the framework was applied to a similar, but larger, prototypical district to quantify the potential benefits of topology optimization. The two prototypical districts considered (heretofore referred to as Numerical Example District for the exhaustive search, and Realistic Application District for the case study) are described in this section.

For both prototypical districts, an energy model in Modelica was used to calculate the energy use associated with a 5GDHC system. Modelica is an equation-based, acausal modeling language that is often used for representing physical systems [25]. The energy model was extended from one developed

Table 1: Summary of values of economic parameters used in LCC calculation

Parameter Name	**Symbol**	**Value**	**Units**	**Source**
Discount rate (%)	NA	3%	NA	[21]
Electricity cost, base year	C_{elec}	27.8	$\frac{\$}{GJ}$	[23]
Natural gas cost, base year	C_{gas}	6.48	$\frac{\$}{GJ}$	[23]
Carbon dioxide cost, base year	C_{CO2}	20.0	$\frac{\$}{mt}$	[24]
Piping and trenching cost	C_{pipes}	548	$\frac{\$}{m}$	[16]

by [21], which was validated using experimental data from a laboratory-scale system at Eurac Research. The DES modeled operated in a two-pipe configuration, with the warm pipe at 26 °C, and the cool pipe at 16 °C. Water-source heat pumps located at each connected load further tempered the water to meet the buildings' heating and cooling loads. The system design facilitates bi-directional thermal and mass flow. A distribution pump located at each load was controlled to maintain a temperature differential of 10 °C across the load. Pipe diameters were selected based on nominal mass flow rates at the district level, and a design nominal flow velocity of 0.15 $\frac{m}{s}$. A central ground-source heat pump controlled the network temperature. A schematic diagram illustrating the system is shown in Figure 2.

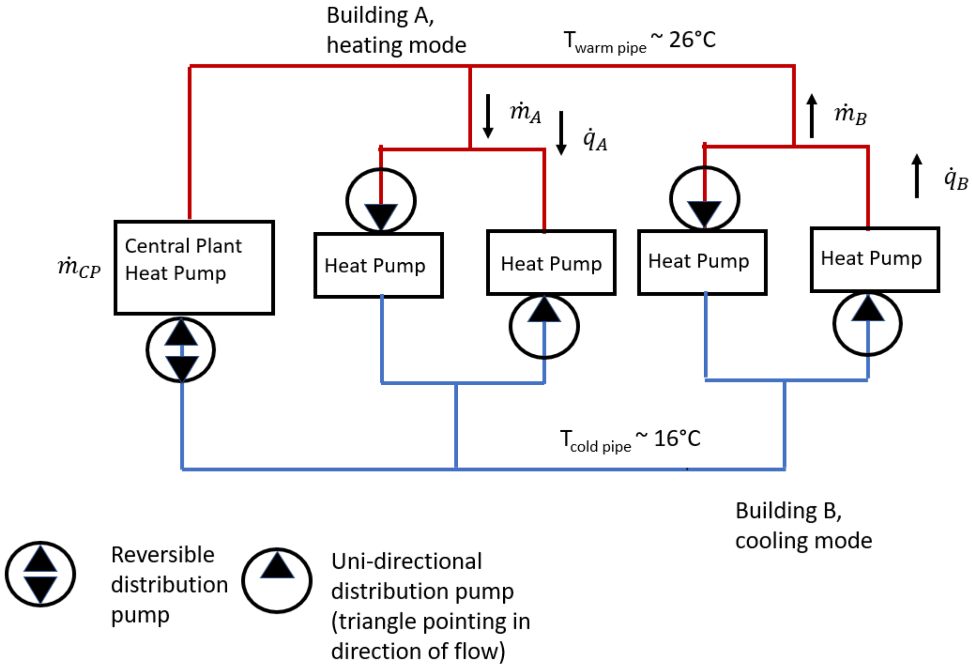

Figure 2: Schematic representation of modeled district thermal energy system, based on a digagram by [26]

For both prototypical districts, the U.S. Department of Energy's Prototype Building Models, which are intended to be representative of the characteristics of common commercial building types in the US, and are available in EnergyPlus format, were used to generate the building load profiles [27]. The Prototype Building Models are adapted from the Commercial Reference Building Models, whose development is documented in [28]. The building types were selected in order to create a sufficient level of thermal load diversity, based on the value of a metric proposed by [29]. Higher levels of thermal load diversity in a district increase the potential level of source EUI reductions from a 5GDHC system [29], due to the ability of connected buildings to offset each other's loads.

Since the LCC calculation includes the HVAC energy use of all buildings in the prototypical district, whether or not they are tied to the DES in a particular scenario, a separate energy model is required to represent each building in its DES-tied and independent cases. In the DES-tied cases, the existing building-level HVAC equipment was replaced with water-source heat pumps. In the independent case, the HVAC systems present in the prototype building models were preserved. Table 3 summarizes attributes of the prototypical buildings considered.[2] In order to integrate the building energy models with the district model in a computationally efficient manner, data-driven metamodels based on the physics-based models were used to represent the building-level HVAC energy use. The Prototype Building models were used to generate a data set over a sweep of parameter values, and random forest models were trained on the data using the Metamodeling Framework developed by [30].

The Numerical Example District consisted of three multifamily buildings, a retail building, and a hospital. For purposes of calculating pipe lengths, these buildings were plotted on an existing block in Golden, Colorado. Figure 3 shows a rendering of the district for illustrative purposes. Note that this district was not intended to represent actual buildings at that location. The Realistic Application District consisted of three office buildings, three multi-family housing buildings, and a restaurant. For purposes of creating a realistic representation of an urban district, the general types and locations

---

[2] Note that the peak heating and cooling loads shown in Table 3 represent space loads only, exclusive of ventilation.

of the buildings are based on those of real buildings located on the University of Colorado Boulder campus. A schematic view of the Realistic Application District is shown in Figure 4. The Supplementary Material offers time series of the buildings' heating and cooling loads as well as further discussion of the energy-use intensity of the prototypical buildings. As part of the case study, the performance, in EUI and LCC, of a DES designed through the use of the framework was compared to that of a system designed based on common metrics used as design heuristics.

A metric based on the ratio of installed heating power to the length of the thermal network required (linear heating power demand density, LHPDD) is often used to screen for techno-economic potential of district heating systems [5]. For the Realistic Application District, the LHPDD is 0.77 $\frac{kW}{m}$, greater than that of some operating 5GDHC systems, as reported by [5]. Based on this evaluation, it is concluded that a DES serving all buildings in the Realistic Application District is a reasonable outcome of a conventional design approach. For the case study evaluation, four different network configurations were considered to represent a conventional design approach, as the base cases: a MST network, ring and radial networks, and a full mesh network, with all possible thermal connections. Ring and radial networks are often used in DES, and the MST and full mesh represent the extremes of network connectivity [21].

2.3. Evaluation of minimal spanning tree heuristic

An exhaustive search, evaluating the LCC of each potential network configuration corresponding to the Numerical Example District, with a total of 30,770 possible configurations, was performed in order to validate the MST heuristic. For each possible subset of connected buildings, the LCC of the MST network was compared to that of all other possible networks to determine if, in fact, the MST corresponded to the least-cost network. There are thirty-two such subsets, including the “null set”, in which all buildings are served by independent systems.

2.4. Evaluation of particle swarm optimization

An implementation of the PSO algorithm was evaluated, through comparison of the solution determined by the algorithm to the ground truth determined by an exhaustive search of all possible scenarios, for the Numerical Example District. This was performed for six cases, distinguished by values of key parameters in the objective function (LCC) , in order to affirm the robustness of the conclusion. Parameter values such as costs for energy and carbon in the objective function effectively weight different components of the LCC, and thus, varying them potentially alters the solution to the problem, making these changes meaningful extensions of the ground truth data set.

For each valid candidate solution, the energy model, in functional mock-up unit (FMU) format, was modified to represent the thermal network connectivity corresponding to the candidate, using the PyFMI Python package. The PyFMI package was then used to simulate the model [31]. The energy consumption values calculated by the simulation, and the static LCC parameter values were then used to calculate the LCC .

2.4.1. Implementation of particle swarm optimization

The formulation of the PSO algorithm for a problem with discrete, binary, variables was implemented, using the PySwarms package in Python [32]. For each of the six sets of LCC parameter values considered, the PSO algorithm was executed for a fixed number of iterations, in order to form a consistent basis of comparison. Based on the work of [13], a threshold for the CV-RMSE of the objective function values for the swarm relative to that of the best objective function thus far was implemented as a convergence criterion.[3] An additional criterion for termination of the algorithm was implemented, based on “stall”, under which the algorithm will terminate if the global best value of the objective function has not improved for a certain number of iterations. In this implementation of PSO, the maximum number of iterations was set at 500, based on the results of several test evaluations.

2.4.2. Selection of life cycle cost parameter values

The six scenarios, distinguished by their parameter values, were selected such that each one resulted in the optimal solution consisting of a different number of buildings served by the thermal network. These parameter values were selected by leveraging a Monte Carlo simulation (MCS) framework for 5GDHC Systems, which will be described in a forthcoming article currently under preparation. The MCS framework performs Monte Carlo analysis varying the values of parameters in the LCC function, to enhance the extensibility of the exhaustive search performed for the Numerical Ex-

---

[3] The CV-RMSE values observed were consistently very low, on the order of 10^{-10}, and did not meaningfully converge.

Table 2: Summary of scenarios for PSO evaluation

Number of connected buildings	Electricity cost $\frac{\$}{kWh}$	Gas cost $\frac{\$}{therm}$	Electricity carbon dioxide emissions intensity $\frac{kg}{kWh}$	Pipe cost $\frac{\$}{m}$
0	0.14	0.57	0.38	922
1	0.15	0.76	0.44	436
2	0.15	1.25	0.75	324
3	0.12	1.20	1.0	311
4	0.11	1.40	0.76	1130
5	0.09	1.20	0.55	815

ample District. Note that the static parameter values shown in Table 1 were used for application to the case study districts.

Parameters related to utility costs–natural gas and electricity rates–were selected to distinguish the scenarios, in addition to the carbon intensity of electricity, and the unit cost of piping and trenching. The considered range of values for the utility costs was selected based on data from the continental U.S. between 2013 and 2018, and for carbon intensity of electricity, for data from the continental U.S. between 1990 and 2018 [23]. The range of values for the unit cost of piping and trenching was selected based on an extensive literature review, including the work of [16], [33], and [19]. The selected values of parameters for these scenarios are shown in Table 2.

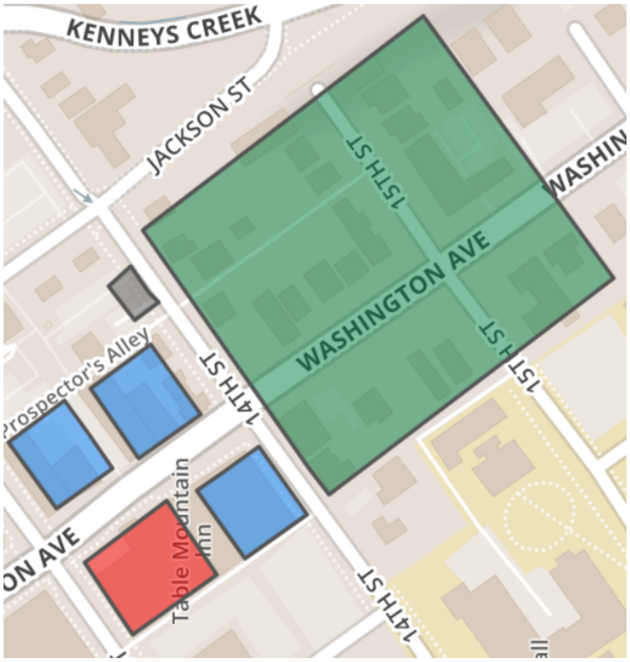

Figure 3: Numerical Example District, with multi-family buildings shown in blue, retail building in red, hospital in green, and central plant in brown.

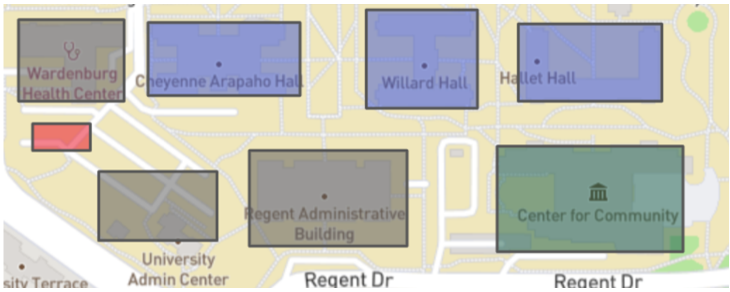

Figure 4: Realistic Application District, with multi-family buildings shown in blue, offices in grey, a restaurant in green, and the central plant in red.

3. Results

Results from the evaluation of the MST heuristic, the PSO implementation, and the application of the framework to a case study are presented in

Table 3: Summary of characteristics of prototypical buildings, including peak heating and cooling loads

Building	Floor Area m^2	Individual HVAC System	Cooling Peak (kW)	Heating Peak (kW)
Hospital	22,436	Variable-air volume reheat system served by water-cooled chillers and hot water boilers	612	514
Multifamily	3,120	Zone-level direct-expansion cooling and gas heating	46.6	30.0
Retail	2,295	Roof-top units with DX cooling and gas heating	70.8	106
Restaurant	510	Roof-top units with DX cooling and gas heating	72.3	72.3

the following sub-sections.

3.1. Evaluation of minimal spanning tree heuristic

For the Numerical Example District, the subset of buildings selected for connection to the DES was greatly influential on the LCC, much more so than the choice of network by which a given subset of buildings was connected.

Inclusion of the prototypical hospital building among the connected buildings is necessary in order for a given scenario to have a lower LCC than that of the "null case", in which all buildings are served by independent systems. The prototypical hospital building had a significantly higher thermal load density than the multi-family or retail buildings, and also has significant internal load diversity. Other studies, including that of [34], have also concluded that higher internal thermal load diversity, as well as higher district-level thermal load diversity, contributes to greater reductions in source EUI for 5GDHC systems relative to independent systems. The hospital is the only building for which a reduction in energy cost occurs with a connection to the DES, though all buildings exhibit at least a slight reduction in site- and source- EUI through a connection to the DES. For the prototypical retail and multi-family buildings, the lower magnitude of this reduction is eclipsed by the higher unit cost of electricity than natural gas. In the independent case, the buildings have natural gas-fired heating systems, while the DES uses only electricity for heating and cooling. There is generally a positive correlation between network length and LCC, due to the fact that the infrastructure cost scales with the network length. The distribution of LCC and source EUI for HVAC exhibited a bifurcation, with the scenarios in which the hospital is served by the DES having a significantly lower LCC and source EUI . Refer to [22] for a figure showing this distribution and to the Supplementary Material for a detailed discussion of the results for source EUI for HVAC.

The exhaustive search confirmed the validity of the MST heuristic. For all possible subsets of buildings in the prototypical district, the network corresponding to the MST indeed provided the solution with the least LCC.

These results were evaluated in terms of an "MST ratio", representing the ratio of the LCC of a given scenario to that of the MST connecting the same subset of buildings. For MST scenarios, the value of this ratio is naturally unity. The fact that this ratio never took on a value less than one demonstrates the validity of the heuristic. Refer to [22] for a figure plotting the MST ratio as a function of network length.

3.2. Evaluation of particle swarm optimization

A summary of results for two of the sets of parameter values considered for the evaluation of PSO are shown in Figure 5. The minimum value in the current swarm and the global minimum thus far, as well as the ground truth value, and the maximum value in the search space, are plotted as a function of the number of iterations. (The scenarios are identified based on the number of connected buildings in the optimal case, with "Scenario 0" corresponding to all buildings having independent systems.) As expected, the global minimum value is monotonically decreasing. In all the scenarios considered, the global best value quickly approached the ground truth value, within the first 100 iterations.

In Scenario 5, the variation in the swarm minima is small compared with the range between the minimum and maximum values of LCC in the search space. In all scenarios, the swarm minimum did not consistently decrease as the algorithm progressed. This behavior is inherent in the structure of the PSO algorithm to balance exploration of the search space with exploitation of a fruitful area. By definition, once the algorithm has identified what is in fact the ground truth solution, it will be impossible to identify a better one,

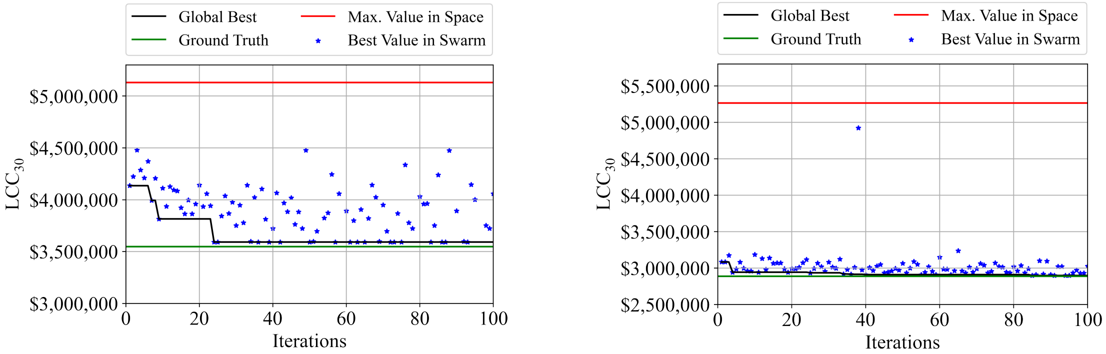

Figure 5: Best values over first 100 iterations for Scenario 0, left, and Scenario 5, right

and the algorithm will continue to explore other areas of the search space. [4]

3.3. Value of topology optimization

For each of the six sets of parameter values considered in the evaluation of PSO, there is a significant range of associated lifetime carbon dioxide emissions and LCC, when statistical outliers are included, as well as significant variation between scenarios. The energy consumption for each case remains the same across scenarios, as the scenarios are distinguished in utility rates, carbon dioxide emissions intensity of electricity, and unit cost of infrastructure. Each of the scenarios represents a set of circumstances that is reasonably likely to occur in the United States, and thus, forms a reasonable basis for quantifying benefits of network topology optimization.

Figure 6 shows boxplots depicting the variation in associated lifetime carbon dioxide emissions and LCC across scenarios and the base case, with the base case characterized by the set of parameter values shown in Table

---

[4] In all cases considered, the algorithm terminated due to the stall criterion being met.

1, from the exhaustive searches performed. The variation in lifetime carbon emissions among the scenarios considered is due to the differing rates of carbon intensity of electricity. The variation in LCC is due to differences in utility rates and infrastructure unit costs, as well as variation in carbon intensity of electricity, which influences the amount of carbon tax accrued. The primary factor contributing to the variation in range of LCC between scenarios is the unit cost of piping and trenching. This parameter takes on its highest value in Scenario 4. For all scenarios, the highest-cost case considered is either a full-mesh network serving all considered buildings, or a network serving all buildings except the prototypical hospital building. This is consistent with results observed for the base case scenario–that the inclusion of a building that experiences a reduction in energy costs due to the use of a district system is necessary, but not always sufficient, in causing a 5GDHC network to be preferable to independent systems on an LCC basis. Figure 8 shows in boxplot form, the range of source EUI for all potential network configurations. The network configuration with the minimum source EUI has a value that is 28% less than that of the maximum source EUI in the search space. Among the six scenarios considered and the base case, the median range of lifetime carbon dioxide emissions is 9.8 megatons, or about 40% of the overall maximum value. Among those same scenarios, the median range of LCC is \$1.64 million, or about 26% of the maximum value.

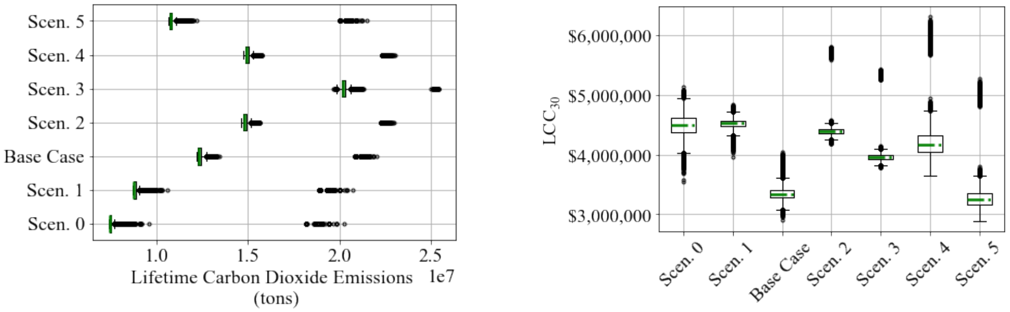

(a) (b)

Figure 6: Boxplots showing the range in carbon dioxide emissions (left) and LCC (right) across scenarios, with median values in green

3.4. Case study

The use of the framework in the context of the Realistic Application District identified network solutions with values of LCC significantly lower than that of the designs based on heuristics. The framework identified four solutions with very similar values of LCC, a value which is 14% lower than that of the best-performing base case (the MST) and 72% lower than that of the worst-performing base case (the full mesh network). Though the objective function considered here does not address potential benefits of resiliency or redundancy of supply, those benefits may, under some circumstances, justify the additional LCC associated with a greater degree of network connectivity. (See the Supplementary Material for a small scale analysis that was performed to address the addition of a constraint in the optimization problem related to redundancy of supply.) Additionally, different configurations of 5GDHC systems, such as those with loads connected in series, may exhibit more pronounced effects on energy consumption associated with greater network connectivity. Characteristics of the optimal solutions determined by

Table 4: Summary of base cases and solutions identified by framework

Scenario	LCC $	Network length (m)	Connected buildings	Source EUI $\frac{MJ}{m2}$
Opt-1	979,867	0	0	176.9
Opt-2	980,377	64	1	170.2
Opt-3	981,602	65	1	170.3
Opt-4	982,381	130	2	163.6
Base-Ring	1,254,779	803	7	141.6
Base-Radial	1,430,558	1,136	7	140.4
Base-Full Mesh	3,500,538	4,924	7	139.4
Base-MST	1,137,870	589	7	141.6

the framework, identified in ascending order of LCC, and of the base case configurations, are shown in Table 4. Design attributes of the DES associated with each solution, where applicable, including maximum pipe diameters, are shown in Table 5. Note that solutions Opt-2 and Opt-3 have very similar values of network length, due to the fact that two of the buildings in the Realistic Application District are almost equidistant from the central plant.

As shown in Table 4, the four optimal solutions identified by the framework consist of a very limited thermal network, or no network at all. Of the four solutions with very similar values of LCC, the solution with the least cost (Opt-1) represents the scenario in which all buildings are served by independent HVAC systems. Recall that the four base case scenarios each entail the connection of all seven buildings to the network. These scenarios

Table 5: Design attributes of base cases and solutions identified by framework

Scenario	Pipe Diameter (m)	Q_{heat} (GJ)	Q_{cool} (GJ)	E_{pump} (GJ)
Opt-1	NA	NA	NA	NA
Opt-2	0.21	132	630	1.88
Opt-3	0.21	138	629	1.87
Opt-4	0.30	270	1,255	3.80
Base-Ring	0.44	964	3,583	20.9
Base-Radial	0.44	977	3,563	9.40
Base-Full Mesh	0.44	1,035	3,326	8.45
Base-MST	0.44	958	3,587	24.5

have very similar values of source EUI, and differ chiefly in terms of the associated network length, which influences the LCC. Ring, radial, and meshed networks can be beneficial in terms of offering resiliency or redundancy of supply. These objectives were not considered in this case, but may be important in some applications. Note also that the optimization search space is constrained to include MST networks only, based on the heuristic validation discussed previously. Thus, full mesh networks were not evaluated as candidate solutions in the optimization process.

The candidate solutions evaluated by the framework offer insight into the attributes influencing the EUI and LCC associated with potential system configurations. Note that these candidate solutions represent a subset of the problem's overall search space, and that the stochastic nature of the

PSO algorithm introduces some randomness into the selection of potential solutions. It is informative to characterize the candidate solutions by the number of connected buildings, because that significantly influences the LCC, a result consistent with the analysis of the Numerical Example District. In this case study, the PSO algorithm converged before evaluating any candidate solutions involving the connection of all seven buildings to the DES. The candidate solutions explored by the optimization algorithm, as well as the base case scenarios, are plotted in Figure 7, in terms of their network length and LCC.

Figure 8 shows, in boxplots, the range of variation in overall LCC, and in the energy and infrastructure components specifically, for the candidate solutions explored by the algorithm and the base case scenarios, grouped by the number of connected buildings. The case in which all buildings are served by independent systems is shown as a single point. (For purposes of concision, the “full mesh” base case scenario, which has a much higher LCC, is not shown on this plot.) A higher number of connected buildings generally results in higher life cycle costs. The use of the district thermal energy system results in lower source EUI relative to independent, building-level systems. In terms of LCC, that effect is dominated by the higher infrastructure costs associated with a thermal network. As shown in the plot on the left in Figure 8, variation in infrastructure cost, driven by the different associated network length, explains most of the variation in LCC among solutions with the same number of connected buildings. The boxplot on the right in Figure 8, showing variation in district-level source EUI, further demonstrates this.

The median source EUI of the four base case scenarios (all of which entail

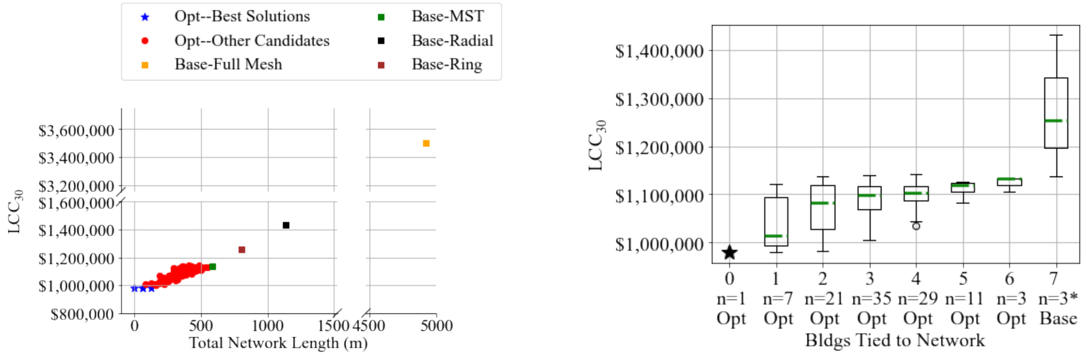

Figure 7: The LCC as a function of network length for base case scenarios and those evaluated by the framework (left) and boxplots showing range of overall LCC as a function of the number of buildings connected to the DES for base case scenarios and those evaluated by the framework (right), with median values in green

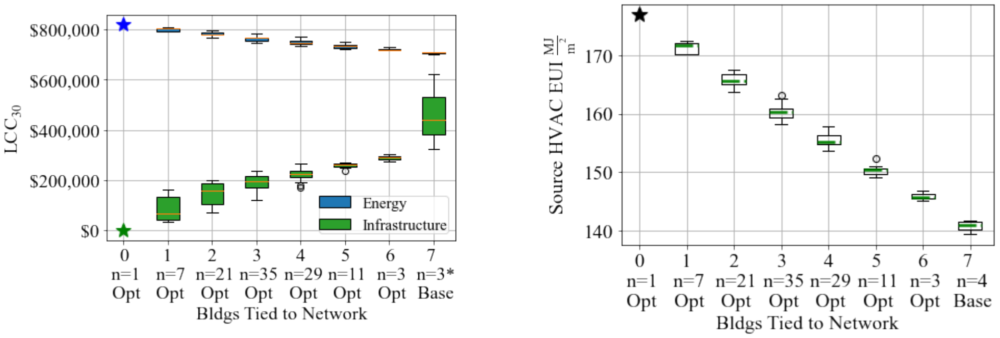

(a)

(b)

Figure 8: Boxplots showing range of overall LCC as a function of the number of buildings connected to the DES for base case scenarios and those evaluated by the framework for energy and infrastructure LCC components (left) and showing range of district-level source EUI for HVAC (right), with median values in green

the connection of all seven buildings to the DES) is 20% lower than that of the null case, in which all buildings are served by independent systems. For intermediate numbers of connected buildings, the district-level source EUI for HVAC is monotonically decreasing between these two values. However, the median energy cost component of the LCC decreases by only 14% (roughly $ 114,500) between the same two points. This is largely the result of the higher cost of meeting a given heating load with electricity as opposed to natural gas, under the rates considered in this study, with electricity having a unit cost 4.3 times that of natural gas. The reduction in energy costs is offset by the increase in infrastructure costs of $ 531,300 between the same two points. The median infrastructure cost also increases monotonically with the number of connected buildings, and is a linear function of the network length.

Each of the building types considered in the Realistic Application District exhibited a reduction in source EUI for HVAC in its DES-connected state. These reductions primarily accrue in heating mode. The centralized ground source heat pump that is modeled as serving the DES operates between an evaporator temperature of 4.4 °C and a condenser temperature of 26 °C in heating, enabling it to achieve an annualized average coefficient of performance (COP) of around 6.0 in heating mode. The building-level heat pumps have nominal COPs in the range of 5.0 to 6.0 for the loop temperatures of 16 °C in cooling and 26 °C in heating. In heating in particular, this represents a significant improvement in exergetic efficiency relative to the 80% efficient gas heating coils serving the independent HVAC systems considered, whose heat loss results in high-temperature exhaust.

4. Discussion

Based on the results of the evaluation of the MST heuristic and PSO, the framework leverages both techniques to address the network topology optimization problem. The optimization problem is formulated as follows:

$$\begin{aligned}\min_{\vec{L}} & C_{pipes} + C_{elec}UPV_{elec}(E_{de} + \sum_{i=1}^{n} E_{be,i}) + C_{gas}UPV_{gas}\sum_{j=1}^{n} E_{bg,j} \\ & + UPV_{CO2}\sum_{t=1}^{30} m_{CO2}(t)C_{CO2}(t)\end{aligned} \tag{2}$$

subject to:

(1) $L_i = 1$ if building i is connected to the DES, and $L_i = 0$ otherwise

(2) If there exists a pipe directly thermally connecting building i and building j, $A_{i,j} = 1$. Otherwise, $A_{i,j} = 0$.

(3) If $\sum_{j=1}^{n+1} \sum_{i=1}^{n+1} A_{i,j} \geq 1, \sum_{j=1}^{n+1} A_{1,j} \geq 1$

(4) $\forall i, j \in \{1 \ldots n+1\}, A_{i,j} = A_{j,i}$.

where $\vec{L}$ is now a vector of $n+1$ dimensions, corresponding to the total number of network nodes considered. The formulation of the problem differs from that in Eqn. 1 due to the reduction in dimensionality of the optimization variable, facilitated by the use of the MST heuristic. Constraint 3 ensures that if any load is connected to the network in a candidate solution, the centralized heat pump is also connected. By definition, an MST network is a connected graph, and thus this constraint is now sufficient to ensure network connectivity. Constraints 2 and 4 are incorporated implicitly, through the approach by which candidate solutions are interpreted in this context. Prim's Algorithm is used to construct the adjacency matrix of the MST graph corresponding to $\vec{L}$ [35]. The application of the MST heuristic significantly reduces the size of the search space, which improves the computational efficiency of the framework.

Analysis of the solution space to the network topology optimization problem revealed that the selection of the subset of buildings to connect to a DES was much more influential on source EUI for HVAC than the network by which they were connected. This result is likely a consequence of the parallel thermal network connections considered in this case, which reduce the potential for localized synergistic exchange of heat among buildings, though building thermal loads still have the potential to offset each other at the network level. This suggests that analysis of other 5GDHC system configurations, such as those with loads connected in series, would demonstrate greater benefits from topology optimization. Future work could address the evaluation of the MST heuristic for 5GDHC systems in which loads are connected in series, which could demonstrate more effects of network topology on energy consumption, due to the greater variation in supply temperature at connected loads.

In the application of the framework to a case study, the four tightly clustered solutions with the least life cycle cost all entailed the absence of a 5GDHC network, or a very limited one. The low cost of natural gas relative to electricity in the US poses a barrier to cost-effective beneficial electrification of heating, and thus, the associated reductions in carbon dioxide emissions. The case study to which the framework was applied sought to represent a generic collection of buildings in an urban area. Location-specific attributes, such as the availability of waste heat from low- and moderate-temperature sources (including data centers and commercial refrigeration), can enhance the cost-effectiveness of 5GDHC systems [36].

5. Conclusion

The significant energy savings potential of 5GDHC systems, and the wide solution space of potential network configurations, motivate improved design approaches for such systems. To advance this, a network Topology Optimization Framework has been developed to select the optimal (with respect to life cycle cost) subset of buildings, if any, to connect to a DES, and the network by which to connect them. The application of the framework to a case study and analysis of realistic values of high-level LCC parameters has revealed:

1. Reductions in source EUI for HVAC of 21-25% through the use of a 5GDHC system, for a typical collection of buildings, relative to code-compliant building-level systems.
2. A median range of carbon dioxide emissions across the scenarios of 40% of the overall maximum value, and a median range of life cycle cost of 26% of the maximum value.
3. Solutions resulting in LCC savings of 14% relative to the best-performing base case, and 72% relative to the worst-performing base case.

Thus, network topology optimization has the potential to facilitate significant reductions in LCC, source EUI, and carbon dioxide emissions. The use of PSO and the MST heuristic by the framework have been validated through the exhaustive search for the Numerical Example District, extended with six different sets of realistic parameter values. This work has addressed buildings with typical space conditioning loads, served by a parallel network configuration. Promising areas for future work in the realm of network topology optimization include the optimal integration of waste heat, which has the potential to improve the economic viability of 5GDHC systems, and evaluation of the MST heuristic in the context of different system configurations.

6. Acknowledgements

A portion of the research was performed using computational resources sponsored by the Department of Energy's Office of Energy Efficiency and Renewable Energy and located at the National Renewable Energy Laboratory. This work was also supported in part by the USA-Ireland Fulbright Scholarship Award.

This work was authored in part by the National Renewable Energy Laboratory, operated by Alliance for Sustainable Energy, LLC, for the U.S. Department of Energy (DOE) under Contract No. DE-AC36-08GO28308. Funding provided by the U.S. Department of Energy Office of Energy Efficiency and Renewable Energy Building Technologies Office. The views expressed herein do not necessarily represent the views of the DOE or the U.S. Government. The U.S. Government retains and the publisher, by accepting the article for publication, acknowledges that the U.S. Government retains a nonexclusive, paid-up, irrevocable, worldwide license to publish or reproduce the published form of this work, or allow others to do so, for U.S. Government purposes.

Nomenclature

Acronyms

5GDHC

fifth-generation district heating and cooling

COP

coefficient of performance

CV-RMSE

coefficient of the variation of the root mean square error

DES

district energy system

DX

direct expansion

EUI

energy use intensity

HVAC

heating, ventilation, and air-conditioning

LCC

life cycle cost

LHPDD

linear heating power demand density

MINLP

mixed-integer non-linear programming problem

MST

minimal spanning tree

PSO

particle swarm optimization

Variables

A

adjacency matrix corresponding to the thermal network

$C_{CO2}(t)$

cost associated with carbon emissions in a given year

C_{pipes}

cost of pipes and trenching

C_{elec}

electricity cost per unit of consumption

C_{gas}

natural gas cost per unit of consumption

$E_{be,i}$

annual electric consumption for HVAC at building i

$E_{bg,j}$

annual natural gas consumption for HVAC at building j

E_{de}

annual electric consumption for the centralized heat pump

$m_{CO2}(t)$

annual carbon emissions in a given year

n

number of buildings considered

UPV_{CO2}

uniform present value factor associated with carbon pricing

UPV_{elec}

uniform present value factor for electricity

UPV_{gas}

uniform present value factor for natural gas

References

[1] E. Larson, C. Greig, J. Jenkins, E. Mayfield, Net-Zero America: Potential Pathways, Infrastructure, and Impacts, 2020.

[2] National Academies of Sciences, Engineering, and Medicine, Accelerating Decarbonization of the U.S. Energy System, 2021.

[3] K. Keramidas, A. Diaz Vazquez, M. Weitzel, Global Energy and Climate Outlook 2019: Electrification for the low-carbon transition, 2019.

[4] Population Division, Department of Economic and Social Affairs, World Urbanization Prospects: The 2018 Revision, United Nations, 2018.

[5] S. Buffa, M. Cozzini, M. D'Antoni, M. Baratieri, R. Fedrizzi, 5th generation district heating and cooling systems: A review of existing cases in Europe, Renewable and Sustainable Energy Reviews 104 (2019). doi:10.1016/j.rser.2018.12.059.

[6] H. Lund, S. Werner, R. Wiltshire, S. Svendsen, J. E. Thorsen, F. Hvelplund, B. V. Mathiesen, 4th Generation District Heating (4GDH). Integrating smart thermal grids into future sustainable energy systems., Energy 68 (2014) 1–11. doi:10.1016/j.energy.2014.02.089. URL `https://www.tandfonline.com/doi/full/10.1080/23744731.2017.1366184`

[7] J. von Rhein, Modeling, Simulation, and Life-Cost Analysis of Fifth-Generation District Heating and Cooling Networks (2018).

[8] F. Bullo, C. Jorge, D. Florian, M. Sonia, Lectures on network systems, Kindle Direct Publishing, 2019.

[9] H. Li, S. Svendsen, District Heating Network Design and Configuration Optimization with Genetic Algorithm, Journal of Sustainable Development of Energy, Water and Environment Systems 1 (4) (2013) 291–303. doi:10.13044/j.sdewes..2013.01.22.

[10] R. N. Sengupta, A. Gupta, J. Dutta, S. Bandaru, K. Deb, CRC Press, 2020.

[11] J. Kennedy, R. Eberhart, Particle swarm optimization, in: Proceedings of ICNN'95 - International Conference on Neural Networks, Vol. 4, 1995, pp. 1942–1948 vol.4. doi:10.1109/ICNN.1995.488968.

[12] C. D. Corbin, G. P. Henze, P. May-Ostendorp, A model predictive control optimization environment for real-time commercial building application, Journal of Building Performance Simulation 6 (3) (2013) 159–174. arXiv:https://doi.org/10.1080/19401493.2011.648343, doi:10.1080/19401493.2011.648343.
URL `https://doi.org/10.1080/19401493.2011.648343`

[13] P. May-Ostendorp, G. P. Henze, C. D. Corbin, B. Rajagopalan, C. Felsmann, Model-predictive control of mixed-mode buildings with rule extraction, Building and Environment 46 (2) (2011) 428 – 437. doi:https://doi.org/10.1016/j.buildenv.2010.08.004.
URL `http://www.sciencedirect.com/science/article/pii/S0360132310002477`

[14] A. P. Engelbrecht, Particle swarm optimization: Global best or local best?, in: 2013 BRICS Congress on Computational Intelligence and 11th Brazilian Congress on Computational Intelligence, 2013, pp. 124–135. doi:10.1109/BRICS-CCI-CBIC.2013.31.

[15] J. Kennedy, R. Eberhart, A discrete binary version of the particle swarm algorithm, in: 1997 IEEE International Conference on Systems, Man, and Cybernetics. Computational Cybernetics and Simulation, Vol. 5, 1997, pp. 4104–4108 vol.5. doi:10.1109/ICSMC.1997.637339.

[16] R. E. Best, P. R. Kalehbasti, M. D. Lepech, A novel approach to district heating and cooling network design based on life cycle cost optimization, Energy 194 (2020) 116837. doi:https://doi.org/10.1016/j.energy.2019.116837.
URL `http://www.sciencedirect.com/science/article/pii/S0360544219325320`

[17] B. Morvaj, R. Evins, J. Carmeliet, Optimising urban energy systems: Simultaneous system sizing, operation and district heating network layout, Energy 116 (2016) 619–636. doi:https://doi.org/10.1016/j.energy.2016.09.139.
URL `https://www.sciencedirect.com/science/article/pii/S0360544216314207`

[18] M. Blommaert, Y. Wack, M. Baelmans, An adjoint optimization approach for the topological design of large-scale district heating networks based on nonlinear models, Applied Energy 280 (2020) 116025. doi:https://doi.org/10.1016/j.apenergy.2020.116025.

URL https://www.sciencedirect.com/science/article/pii/S0306261920314653

[19] T. Mertz, S. Serra, A. Henon, J. M. Reneaume, A MINLP optimization of the configuration and the design of a district heating network: Academic study cases, Energy 116 (2016) 236–248. doi:10.1016/j.egypro.2017.05.071.

[20] T. Falke, S. Krengel, A. K. Meinerzhagen, A. Schnettler, Multi-objective optimization and simulation model for the design of distributed energy systems, Applied Energy 184 (2016) 1508–1516. doi:10.1016/j.apenergy.2016.03.044.
URL http://dx.doi.org/10.1016/j.apenergy.2016.03.044

[21] J. von Rhein, G. P. Henze, N. Long, Y. Fu, Development of a topology analysis tool for fifth-generation district heating and cooling networks, Energy Conversion and Management 196 (March) (2019) 705–716. doi:10.1016/j.enconman.2019.05.066.
URL https://doi.org/10.1016/j.enconman.2019.05.066

[22] A. Allen, G. Henze, K. Baker, G. Pavlak, M. Murphy, Evaluation of Topology Optimization to Achieve Energy Savings at the Urban District Level, Vol. 127, ASHRAE, 2021, p. 537–547.

[23] U.S. Energy Information Administration, U.S. Energy Information Administration - EIA - Independent Statistics and Analysis, [Accessed 14/02/2020] (2019).
URL https://www.eia.gov/electricity/?t=epmt56a

[24] P. D. Lavappa, J. D. Kneifel, Energy Price Indices and Discount Factors for Life-Cycle Cost Analysis – 2019 Annual Supplement to NIST Handbook 135, National Institute of Standards and Technology . U.S Depatrtement of Commerce (NISTIR 85-3273-34) (2019) 67.

[25] Modelica language.
URL `https://www.modelica.org/modelicalanguage`

[26] M. Wetter, J. Hu, Quayside Energy Systems Analysis (2019).

[27] U.S. Department of Energy, Commercial prototype building models.
URL `\url{https://www.energycodes.gov/development/commercial/prototype\_models}`

[28] M. Deru, K. Field, D. Studer, U.S. Department of Energy Commercial Reference Building Models of the National Building Stock, 2011.

[29] R. Zarin Pass, M. Wetter, M. A. Piette, A thermodynamic analysis of a novel bidirectional district heating and cooling network, Energy 144 (2018) 20–30. doi:10.1016/j.energy.2017.11.122.

[30] N. Long, Reduced Order Models for Rapid Analysis of Ambient Loops for Commercial Buildings, Ph.D. thesis, University of Colorado Boulder, Boulder, CO (2018).

[31] Modelon AB, PyFMI (2018).

[32] L. J. Miranda, Pyswarms: a research toolkit for particle swarm optimization in python, Journal of Open Source Software 3 (21) (2018) 433.

doi:10.21105/joss.00433.
URL `https://doi.org/10.21105/joss.00433`

[33] F. Marty, S. Serra, S. Sochard, J.-M. Reneaume, Simultaneous optimization of the district heating network topology and the organic rankine cycle sizing of a geothermal plant, Energy 159 (2018) 1060 – 1074. doi:https://doi.org/10.1016/j.energy.2018.05.110.
URL `http://www.sciencedirect.com/science/article/pii/S0360544218309368`

[34] M. Wirtz, L. Kivilip, P. Remmen, D. Müller, Quantifying demand balancing in bidirectional low temperature networks, Energy and Buildings 224 (2020) 110245. doi:https://doi.org/10.1016/j.enbuild.2020.110245.
URL `https://www.sciencedirect.com/science/article/pii/S0378778820309889`

[35] J. Morris (1998). [link].
URL `https://www.cs.auckland.ac.nz/software/AlgAnim/prim.html`

[36] H. Fang, J. Xia, K. Zhu, Y. Su, Y. Jiang, Industrial waste heat utilization for low temperature district heating, Energy Policy 62 (2013) 236–246.

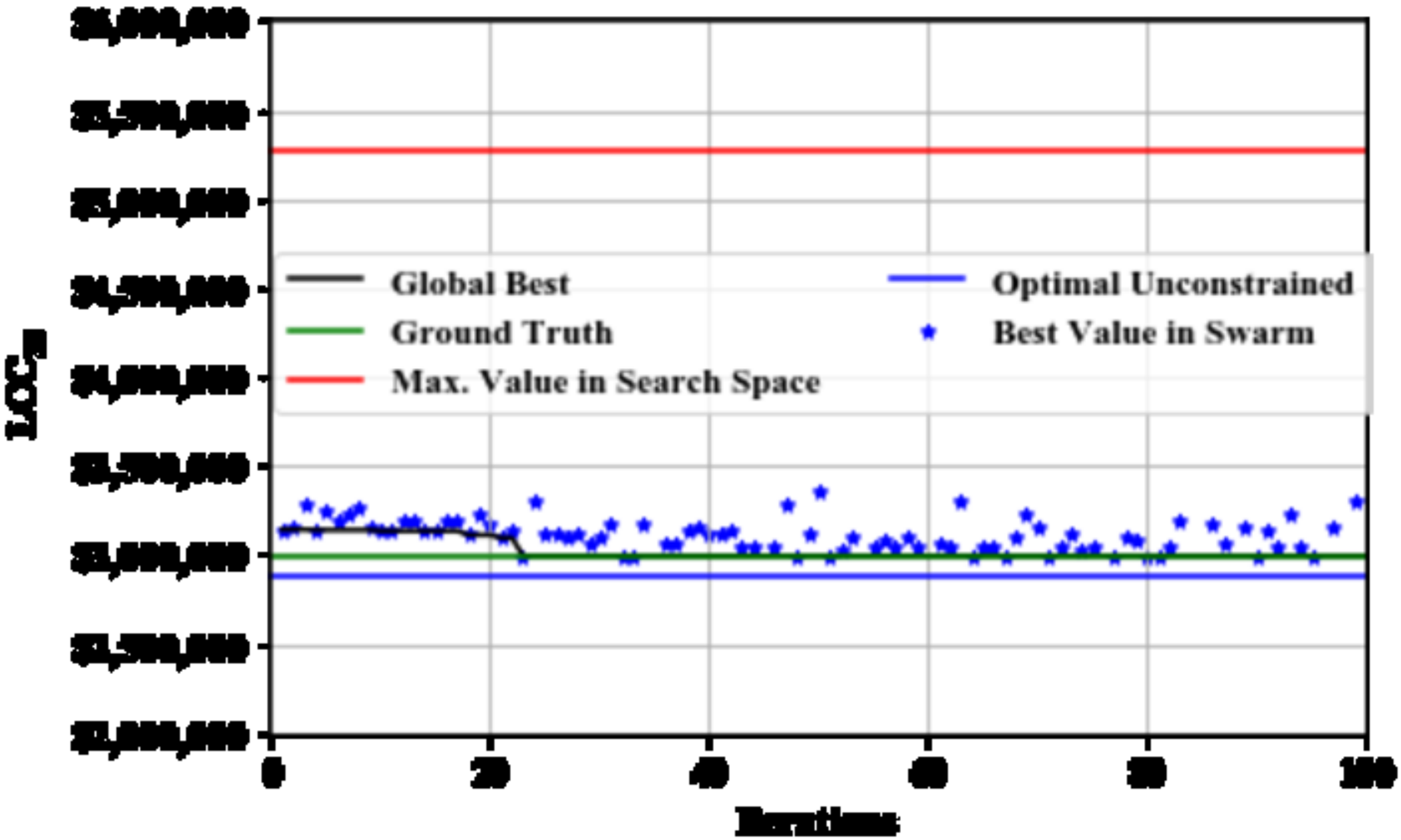
Global Best
Ground Truth
Max. Value in Search Space
Optimal Unconstrained
Best Value in Swarm
LCC
0
20
40
60
80
100
Iterations

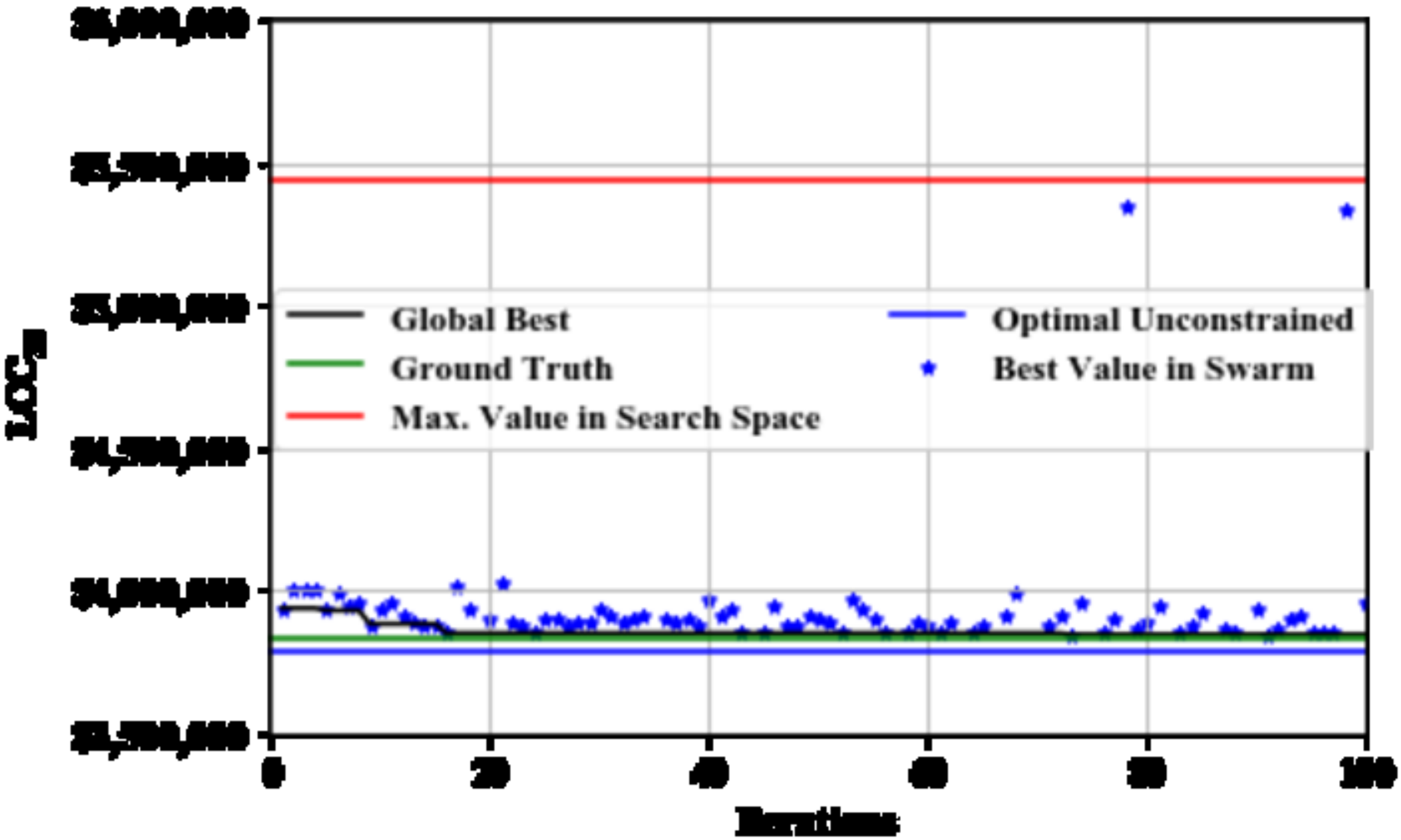
LCC
Iterations
0
20
40
60
80
100
Global Best
Ground Truth
Max. Value in Search Space
Optimal Unconstrained
Best Value in Swarm

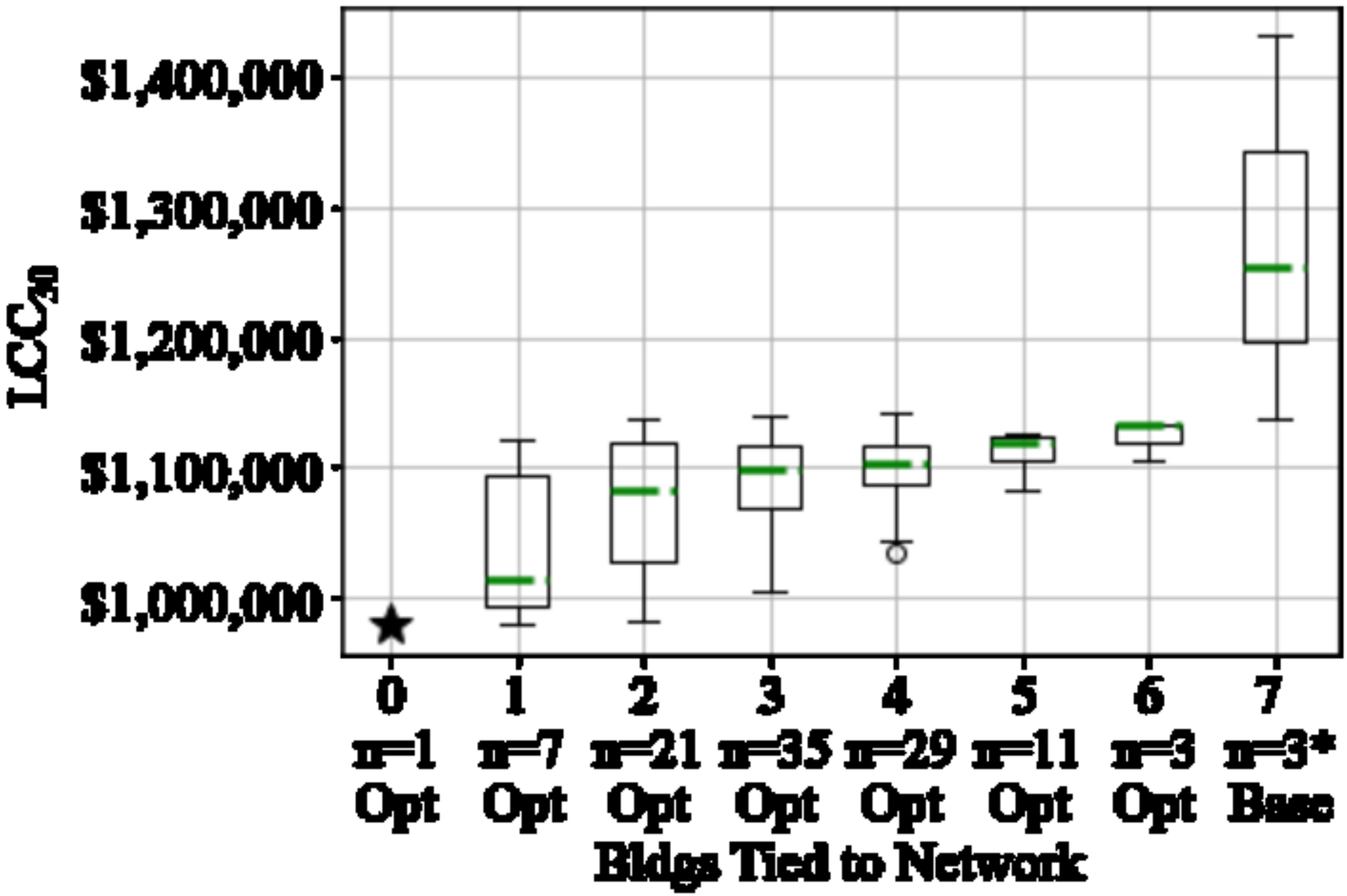
$1,400,000
$1,300,000
$1,200,000
$1,100,000
$1,000,000
LCC30
0
n=1
Opt
1
n=7
Opt
2
n=21
Opt
3
n=35
Opt
4
n=29
Opt
5
n=11
Opt
6
n=3
Opt
7
n=3*
Base
Bldgs Tied to Network

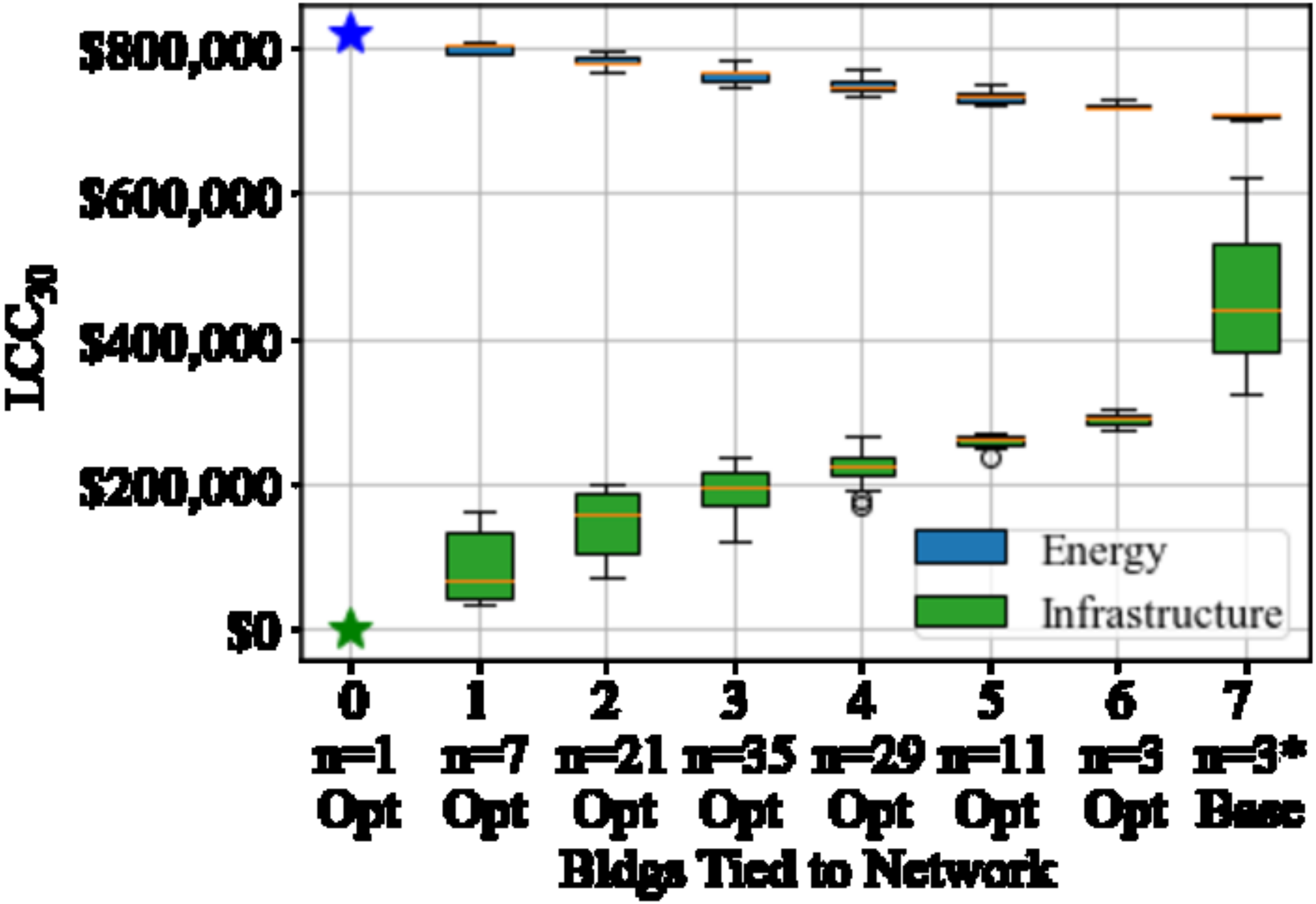
$800,000
$600,000
$400,000
$200,000
$0
LCC30
Energy
Infrastructure
0 n=1 Opt
1 n=7 Opt
2 n=21 Opt
3 n=35 Opt
4 n=29 Opt
5 n=11 Opt
6 n=3 Opt
7 n=3* Base
Bldgs Tied to Network

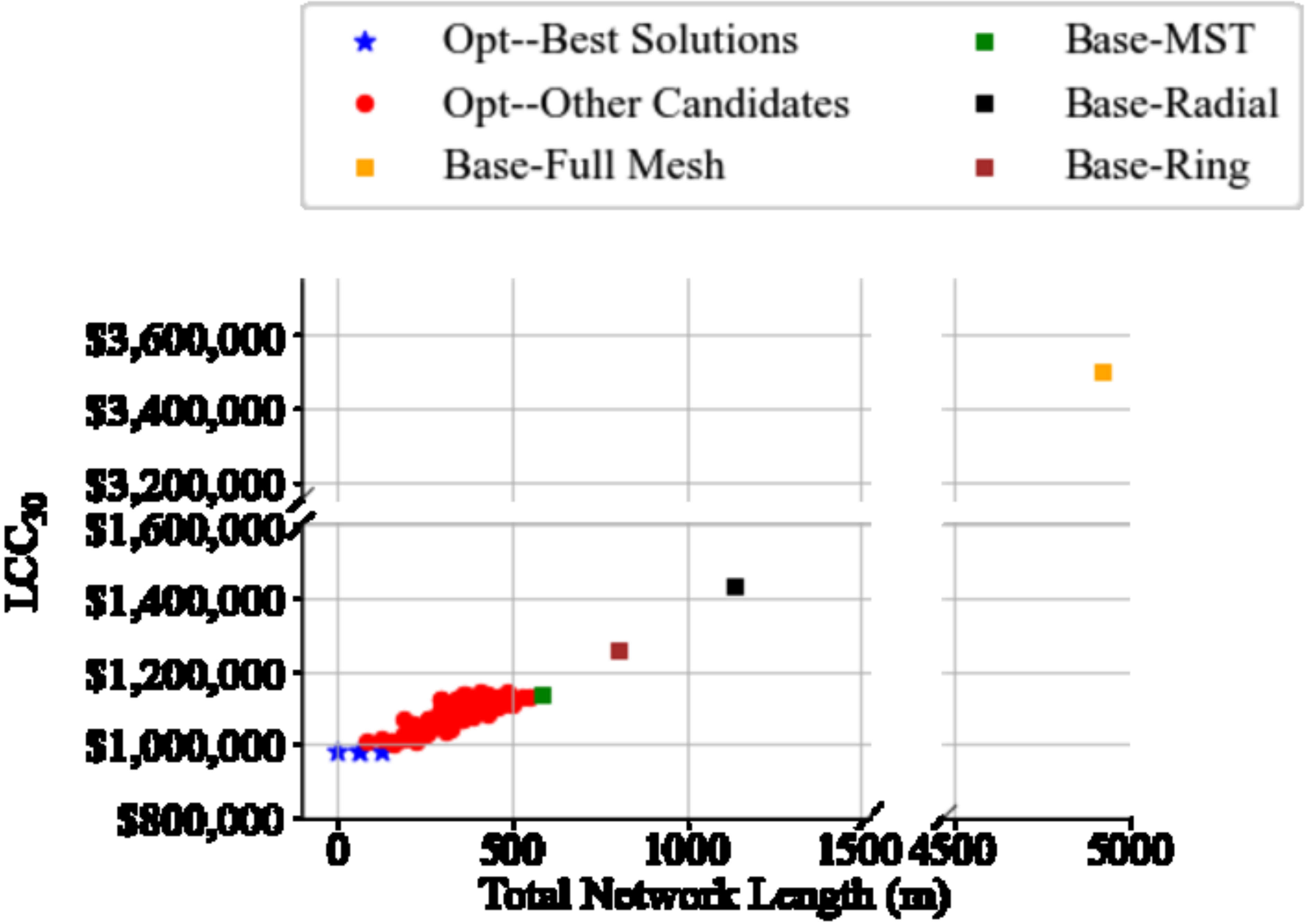
Opt--Best Solutions
Opt--Other Candidates
Base-Full Mesh
Base-MST
Base-Radial
Base-Ring
$3,600,000
$3,400,000
$3,200,000
$1,600,000
$1,400,000
$1,200,000
$1,000,000
$800,000
LCC$_{30}$
0
500
1000
1500
4500
5000
Total Network Length (m)

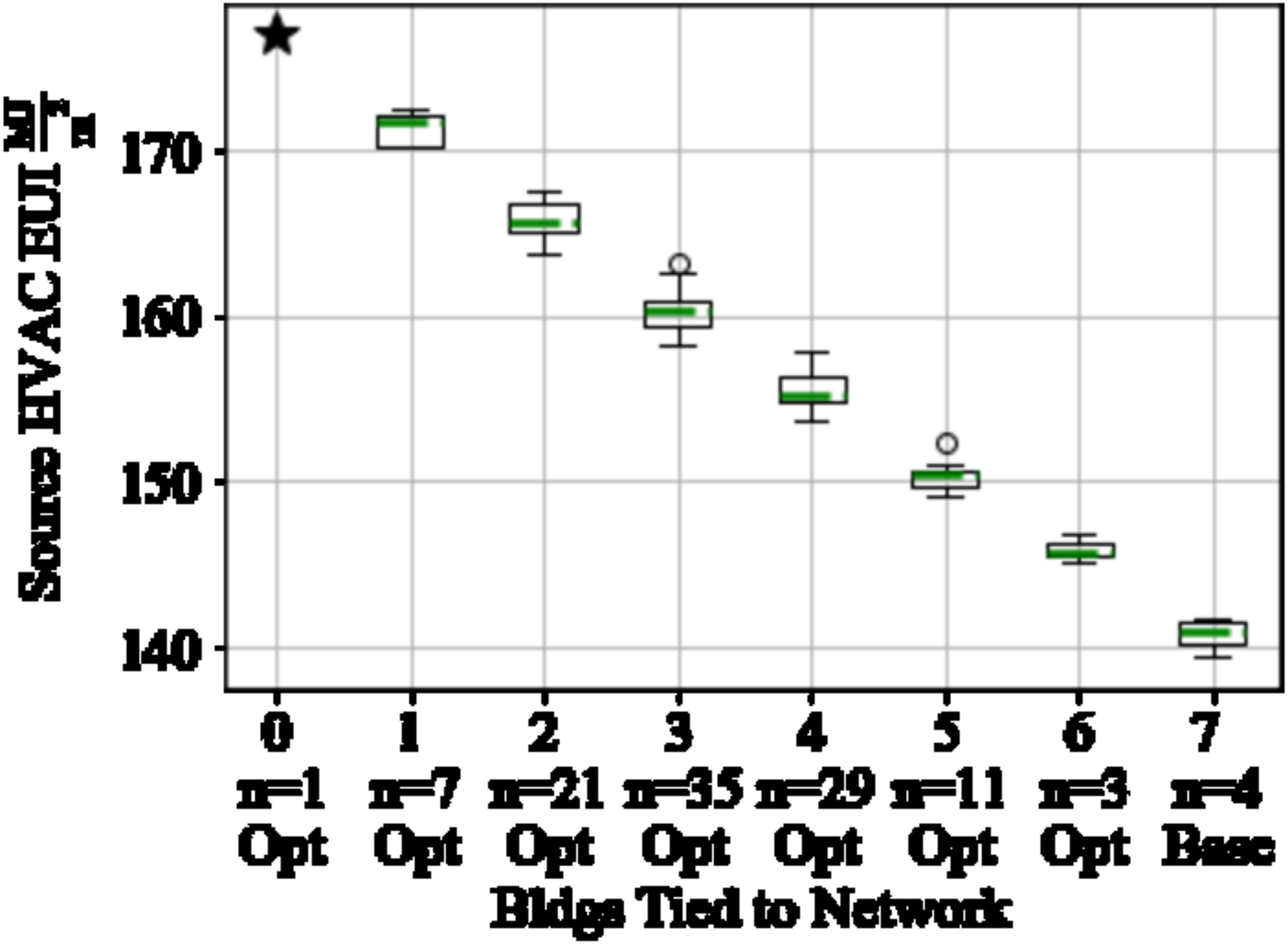
Source HVAC EUI $\frac{MJ}{m^2}$
170
160
150
140
0
n=1
Opt
1
n=7
Opt
2
n=21
Opt
3
n=35
Opt
4
n=29
Opt
5
n=11
Opt
6
n=3
Opt
7
n=4
Base
Bldgs Tied to Network

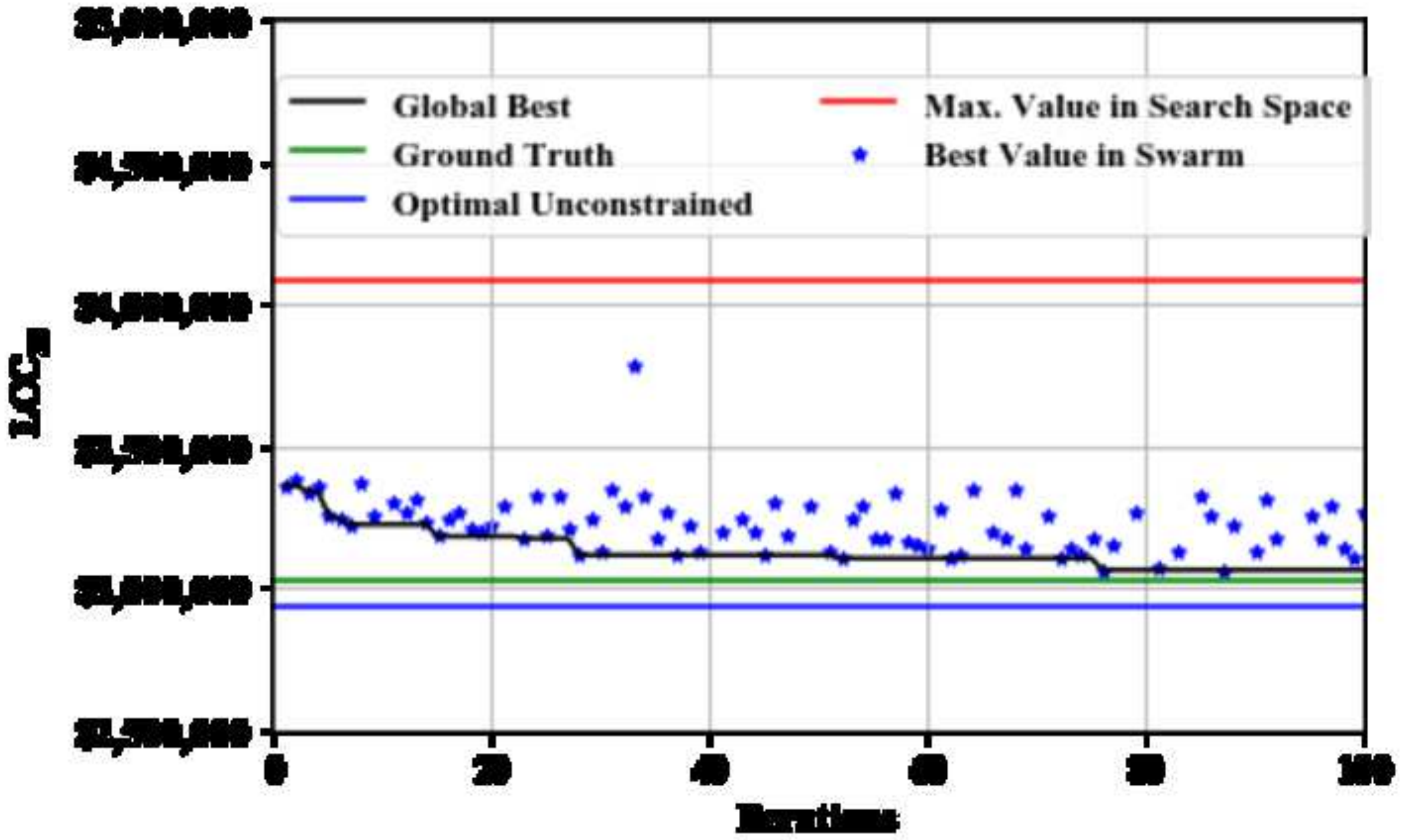
Global Best
Ground Truth
Optimal Unconstrained
Max. Value in Search Space
Best Value in Swarm
$5,000,000
$4,500,000
$4,000,000
$3,500,000
$3,000,000
$2,500,000
0
20
40
60
80
100
Iterations

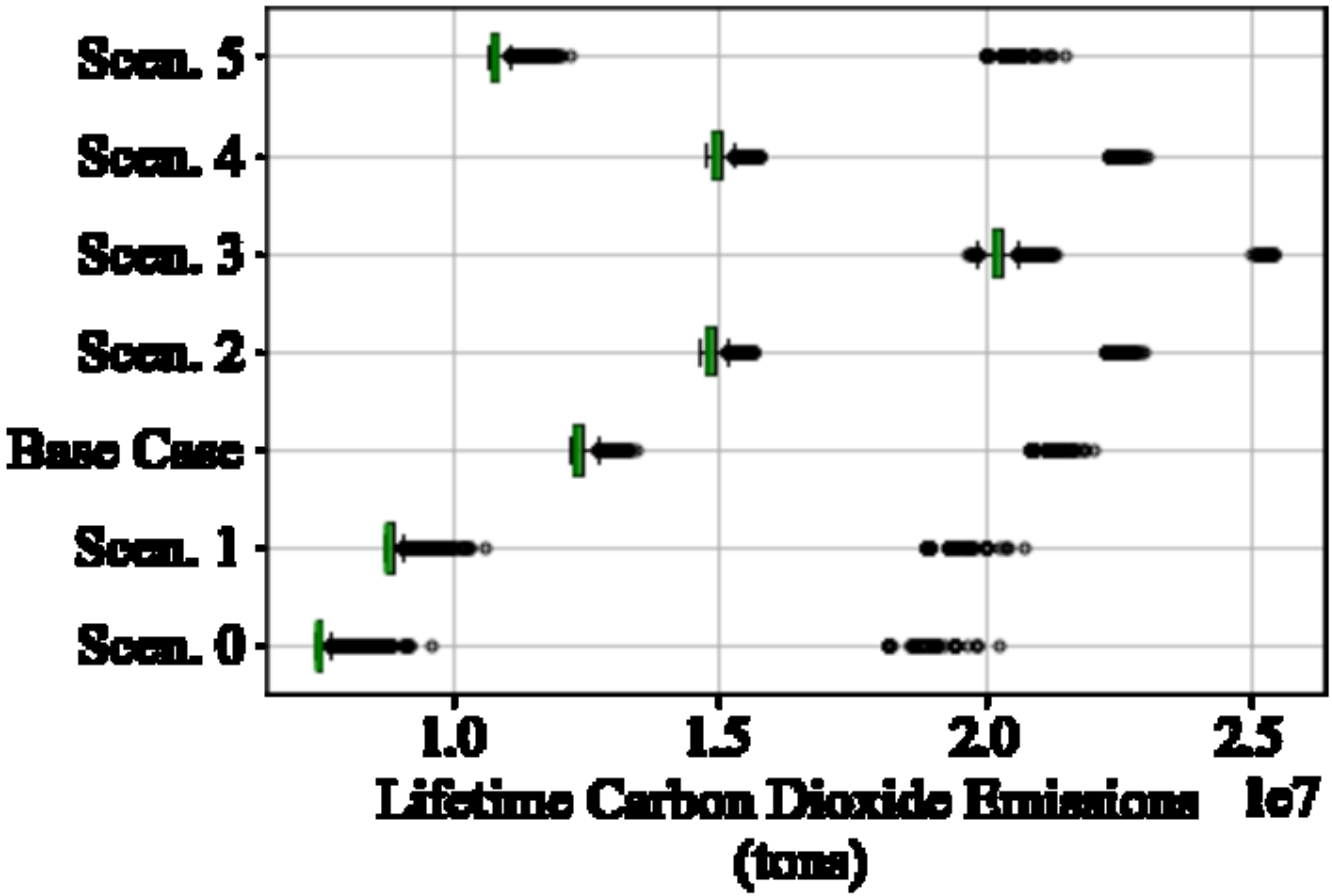
Scen. 5
Scen. 4
Scen. 3
Scen. 2
Base Case
Scen. 1
Scen. 0
1.0
1.5
2.0
2.5
Lifetime Carbon Dioxide Emissions (tons)
1e7

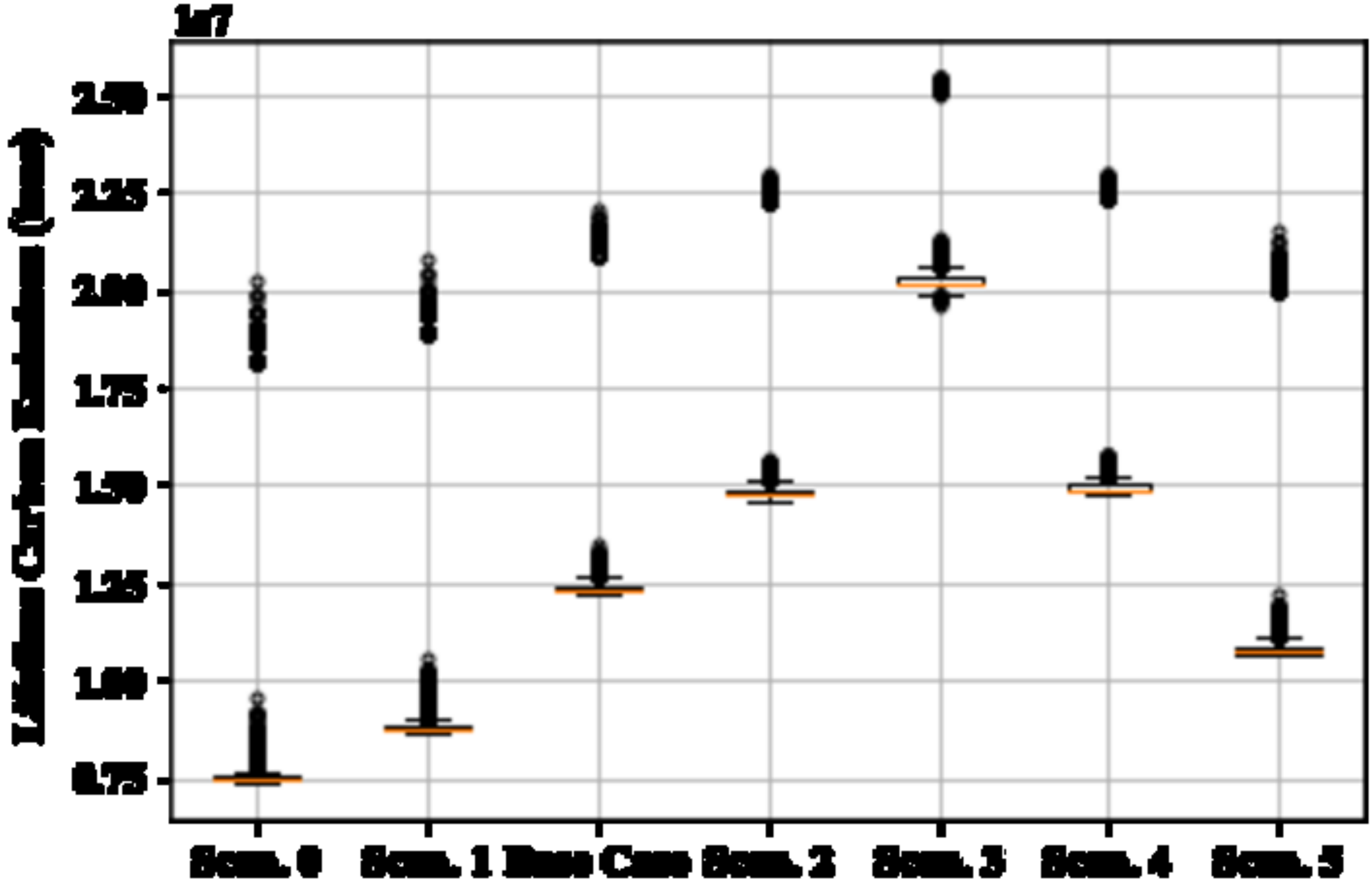
1e7
2.50
2.25
2.00
1.75
1.50
1.25
1.00
0.75
Scen. 0
Scen. 1
Base Case
Scen. 2
Scen. 3
Scen. 4
Scen. 5

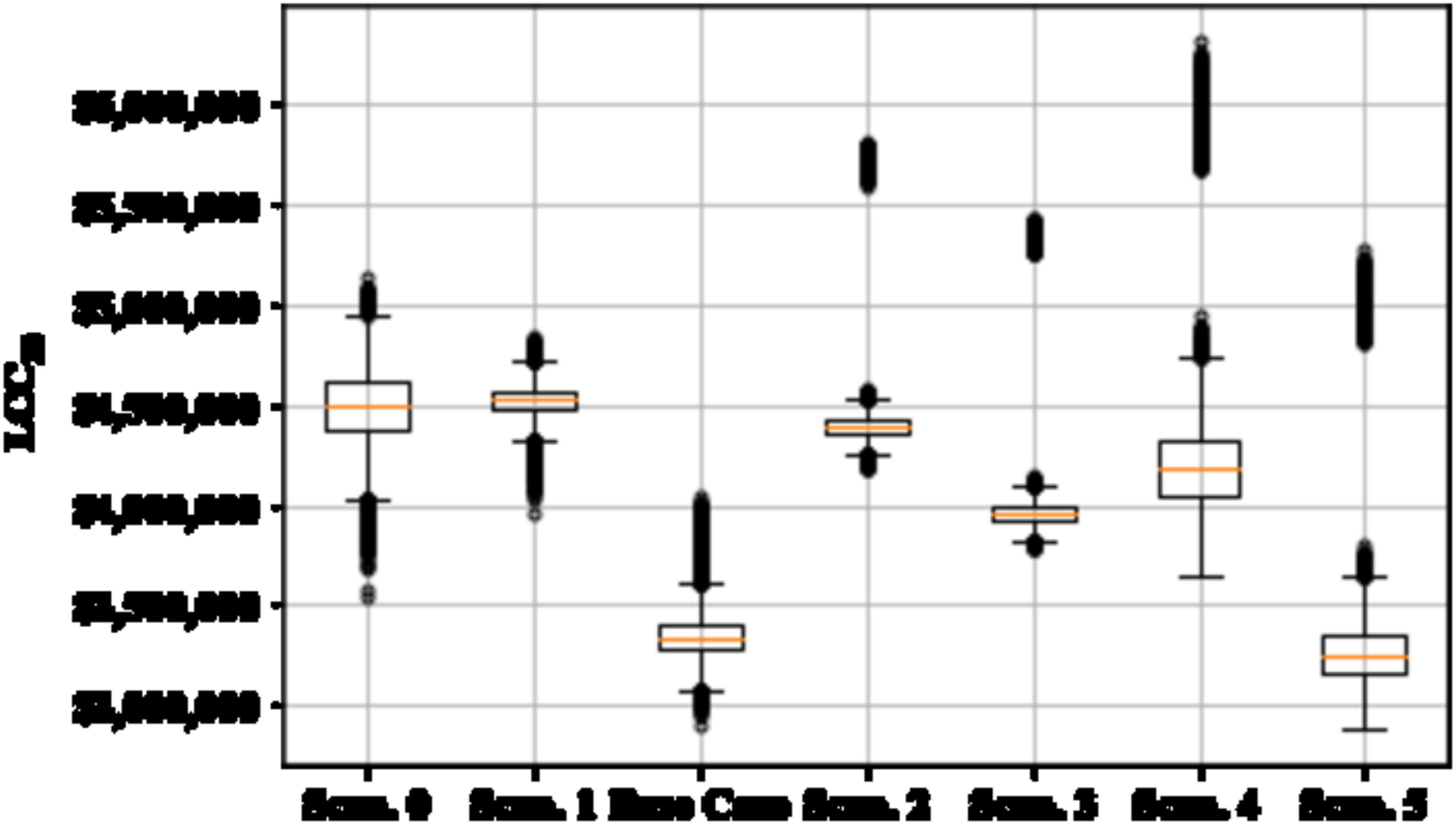
$36,000,000
$35,500,000
$35,000,000
$34,500,000
$34,000,000
$33,500,000
$33,000,000
LCC$_s$
Scen. 0
Scen. 1
Base Case
Scen. 2
Scen. 3
Scen. 4
Scen. 5

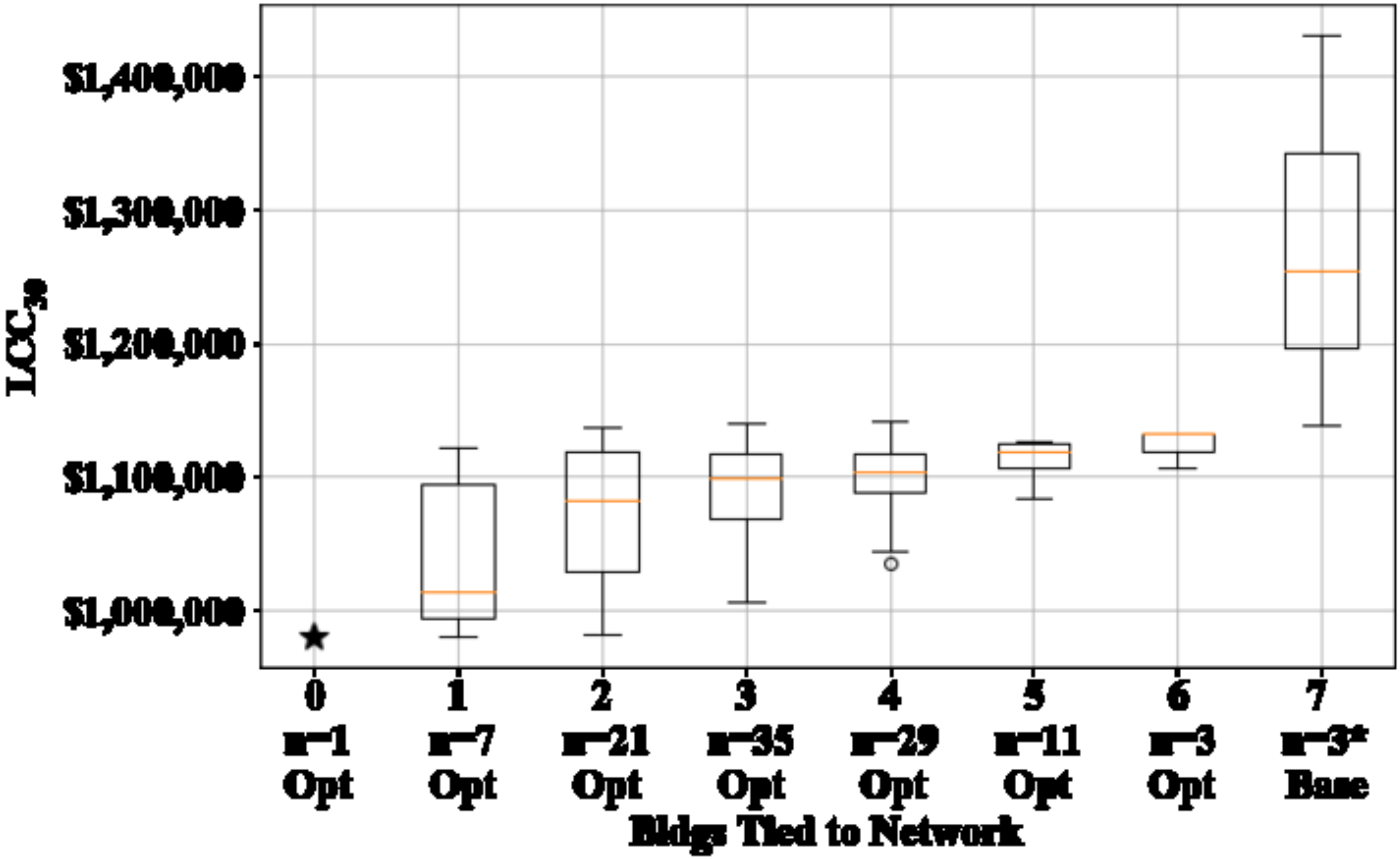
$1,400,000
$1,300,000
$1,200,000
$1,100,000
$1,000,000
LCC30
0
n=1
Opt
1
n=7
Opt
2
n=21
Opt
3
n=35
Opt
4
n=29
Opt
5
n=11
Opt
6
n=3
Opt
7
n=3*
Base
Bldgs Tied to Network

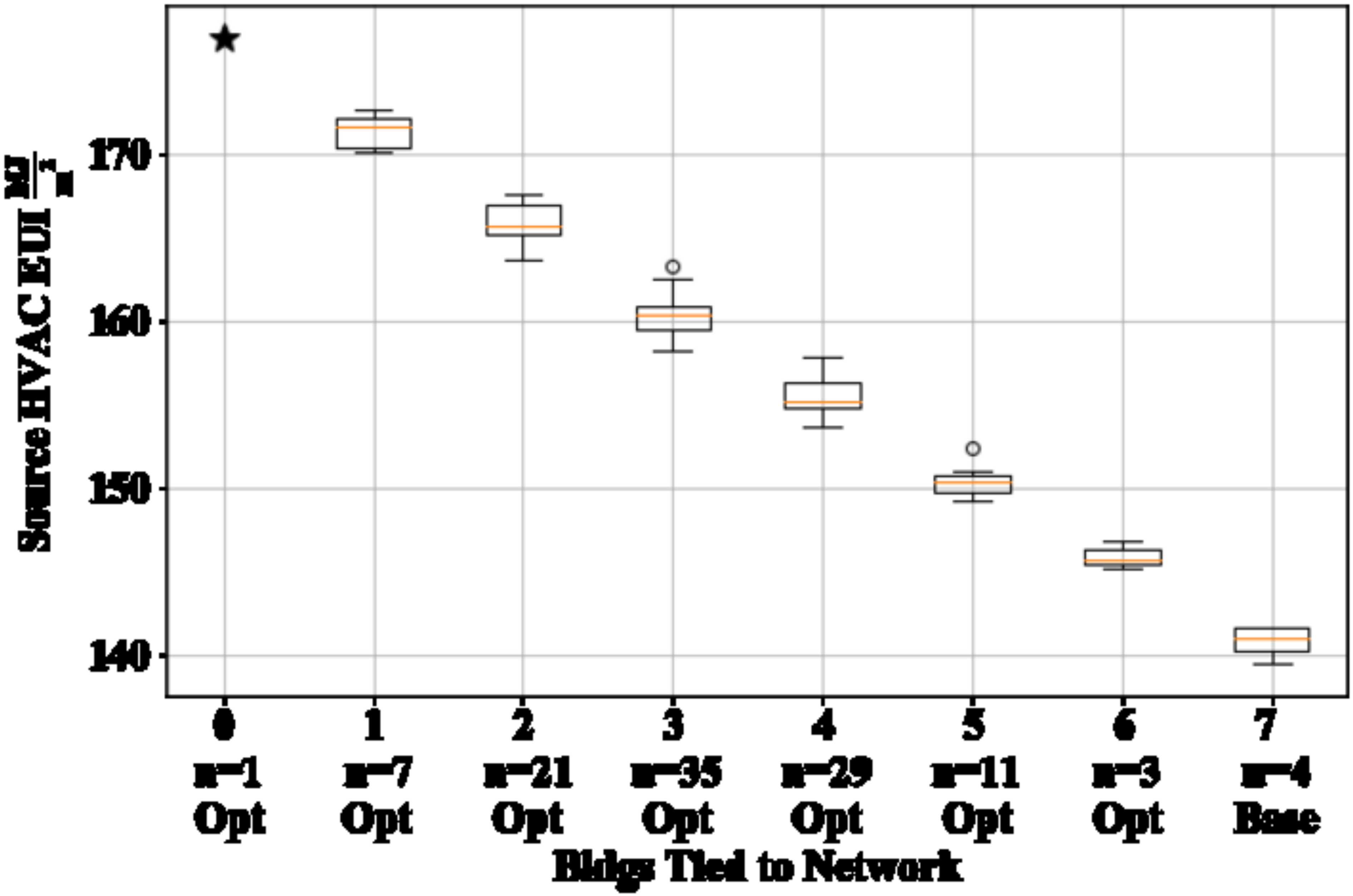
Source HVAC EUI $\frac{MJ}{m^2}$
170
160
150
140
0
n=1
Opt
1
n=7
Opt
2
n=21
Opt
3
n=35
Opt
4
n=29
Opt
5
n=11
Opt
6
n=3
Opt
7
n=4
Base
Bldgs Tied to Network

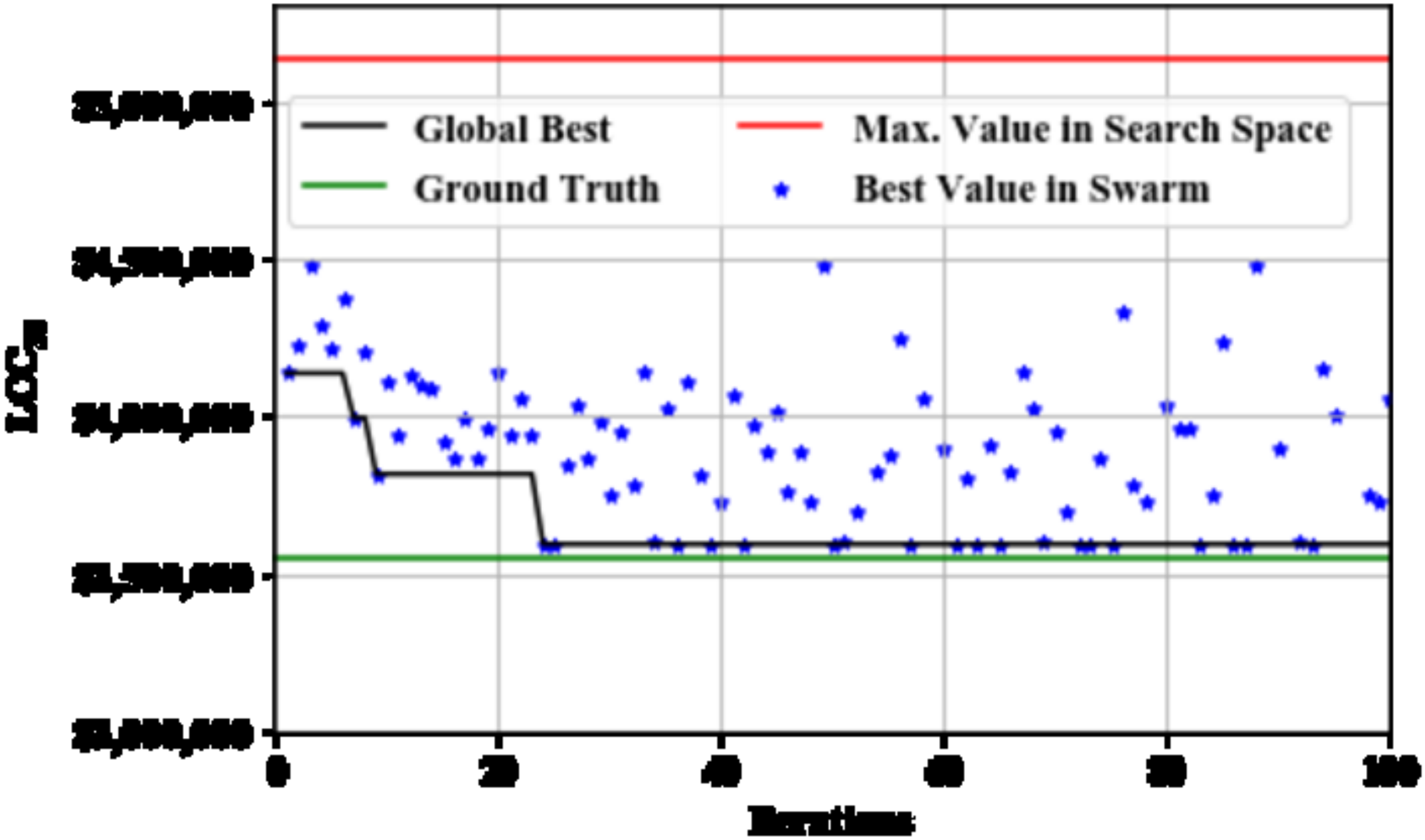
Global Best
Ground Truth
Max. Value in Search Space
Best Value in Swarm
$5,000,000
$4,500,000
$4,000,000
$3,500,000
$3,000,000
LCC
0
20
40
60
80
100
Iterations

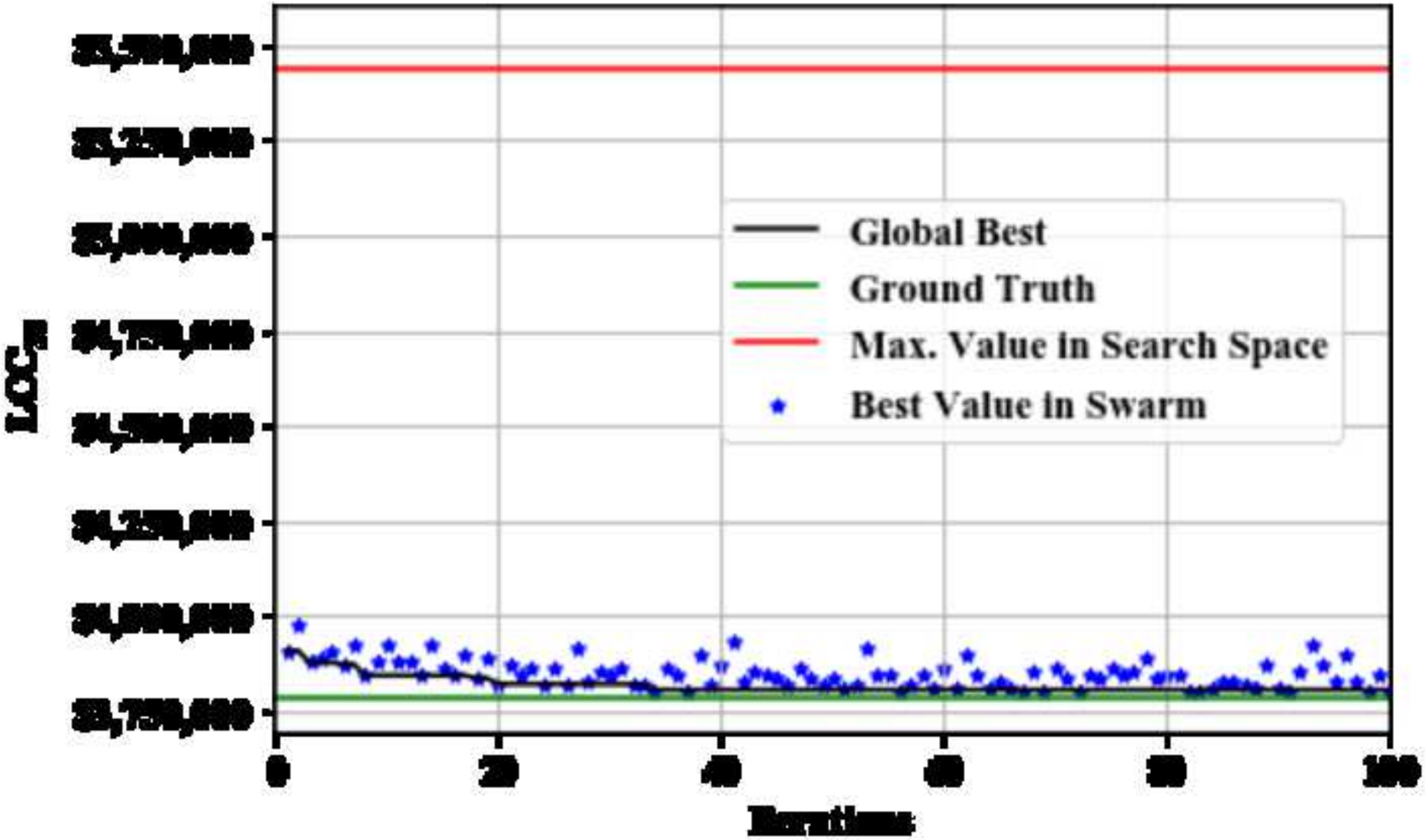
35,500,000
35,250,000
35,000,000
34,750,000
34,500,000
34,250,000
34,000,000
33,750,000
LCC_B
0
20
40
60
80
100
Iterations
Global Best
Ground Truth
Max. Value in Search Space
Best Value in Swarm

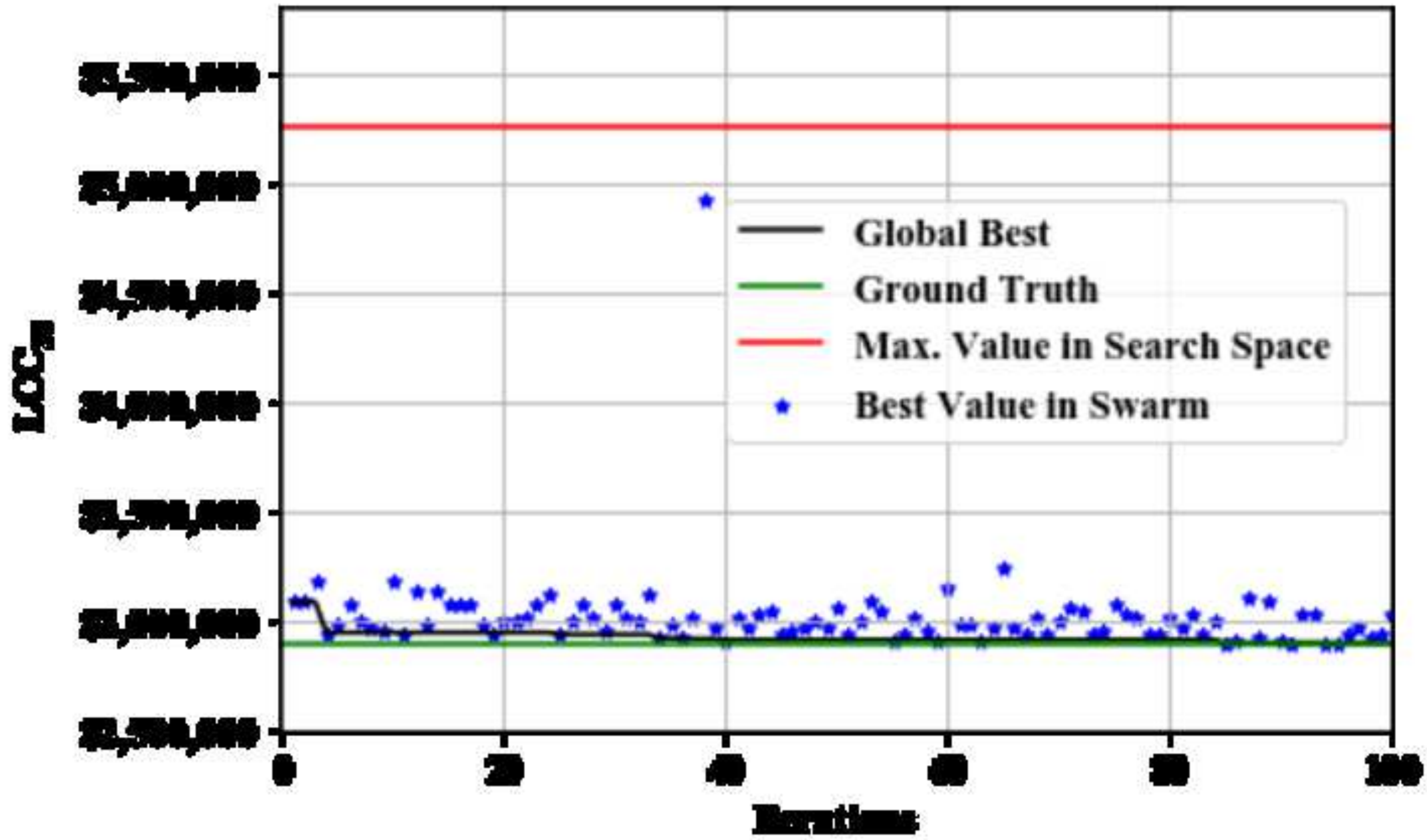
$35,500,000
$35,000,000
$34,500,000
$34,000,000
$33,500,000
$33,000,000
$32,500,000
LCC
0
20
40
60
80
100
Iterations
Global Best
Ground Truth
Max. Value in Search Space
Best Value in Swarm

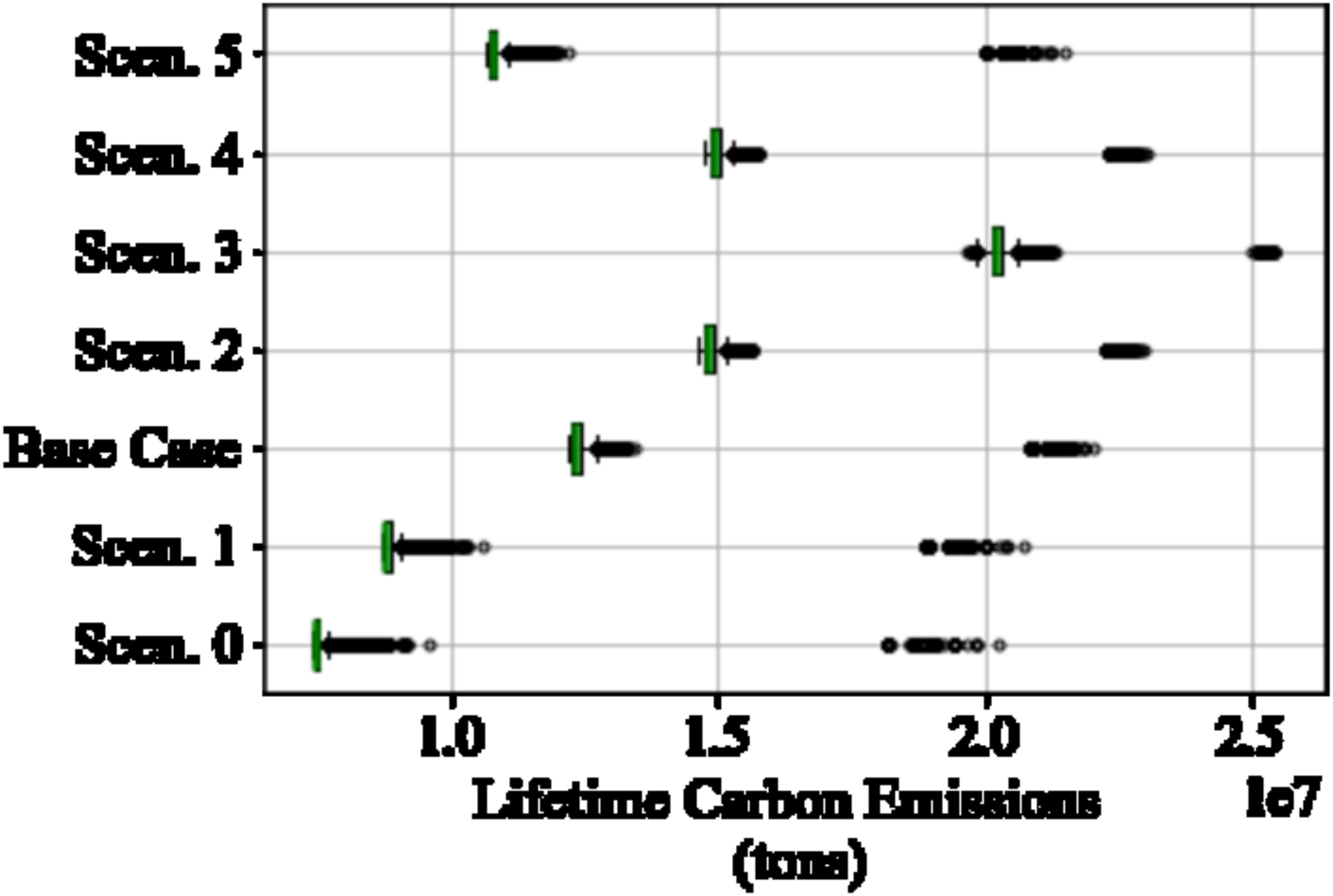
Scen. 5
Scen. 4
Scen. 3
Scen. 2
Base Case
Scen. 1
Scen. 0
1.0
1.5
2.0
2.5
1e7
Lifetime Carbon Emissions (tons)

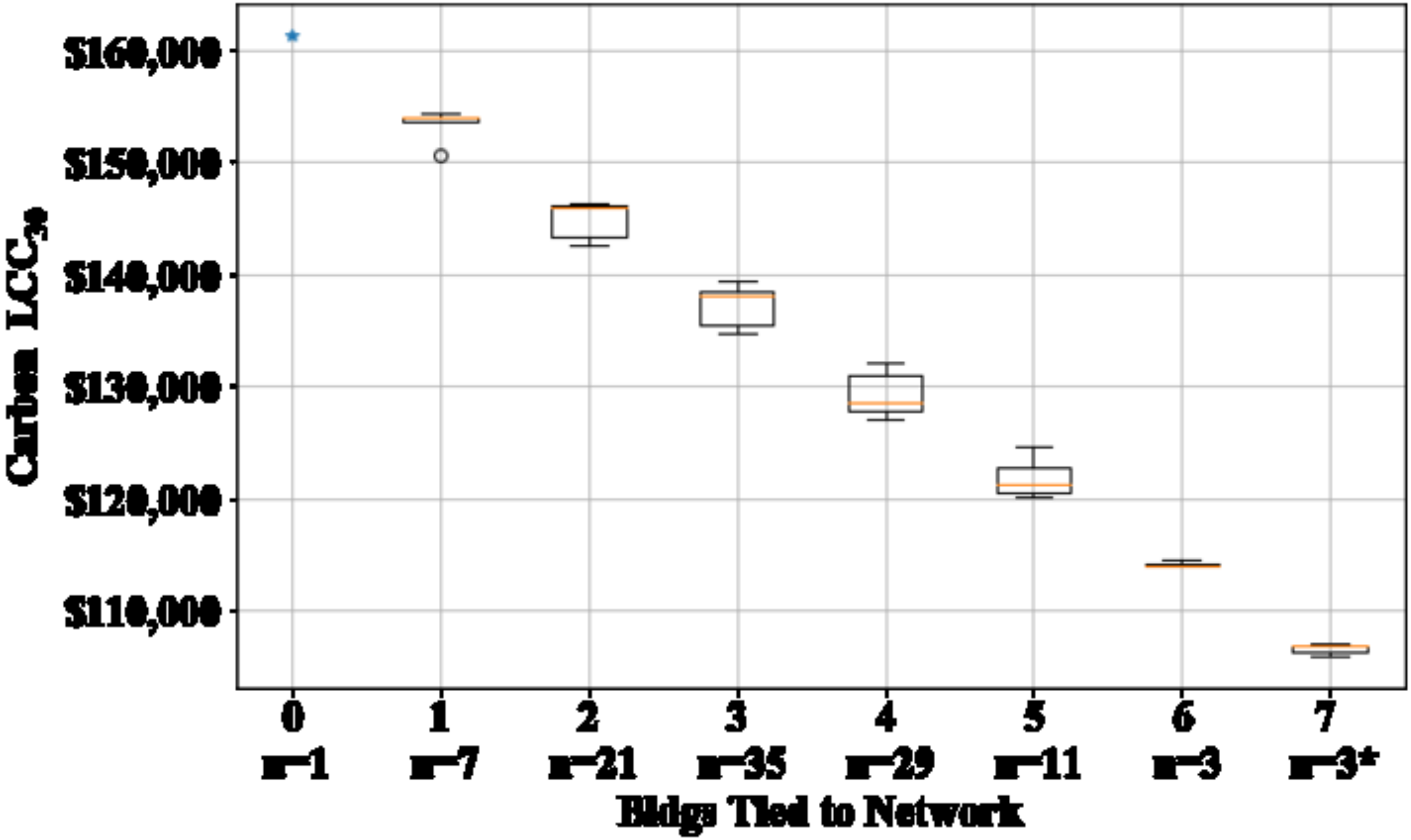
$160,000
$150,000
$140,000
$130,000
$120,000
$110,000
Carbon LCC$_{30}$
0
n=1
1
n=7
2
n=21
3
n=35
4
n=29
5
n=11
6
n=3
7
n=3*
Bldgs Tied to Network

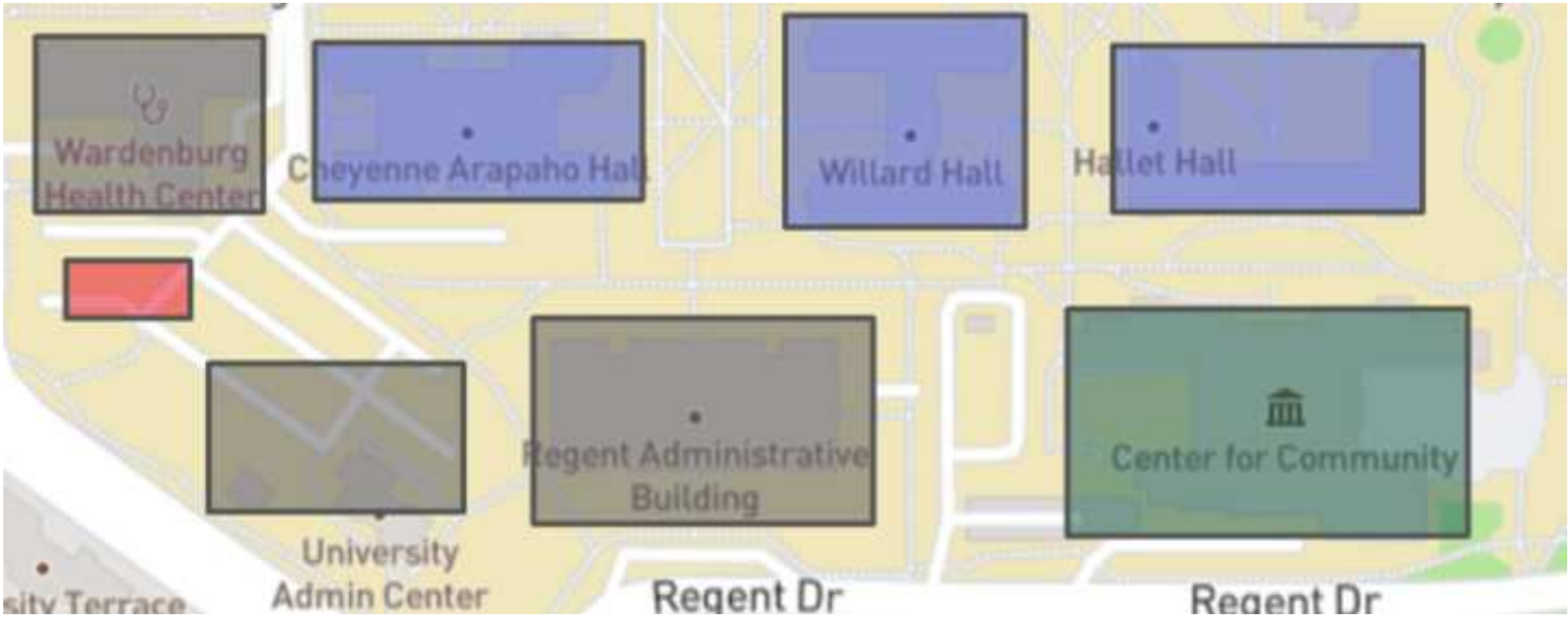
Wardenburg Health Center
Cheyenne Arapaho Hall
Willard Hall
Hallet Hall
Regent Administrative Building
Center for Community
University Admin Center
sity Terrace
Regent Dr
Regent Dr

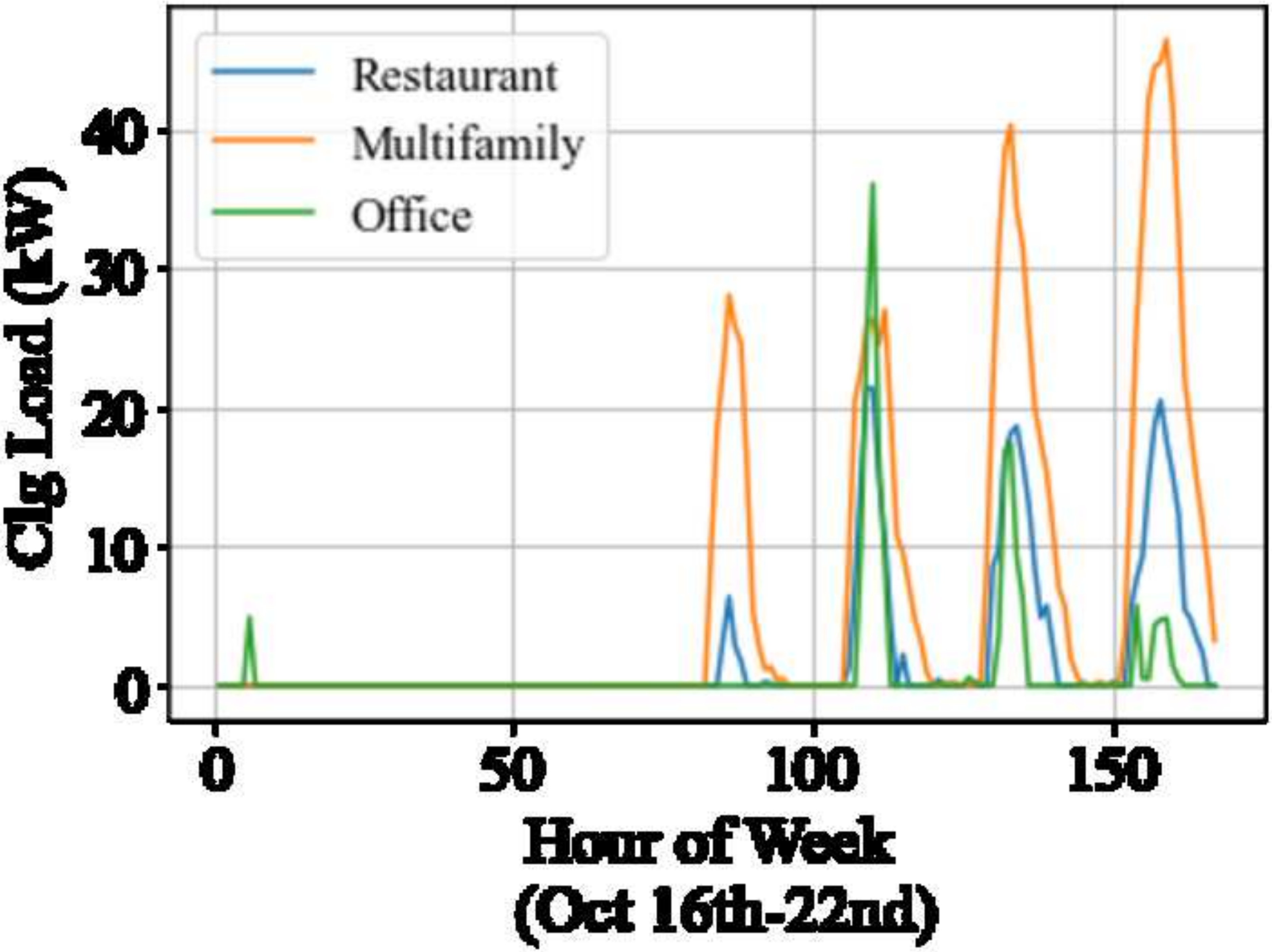
Restaurant
Multifamily
Office
Clg Load (kW)
0
10
20
30
40
0
50
100
150
Hour of Week
(Oct 16th-22nd)

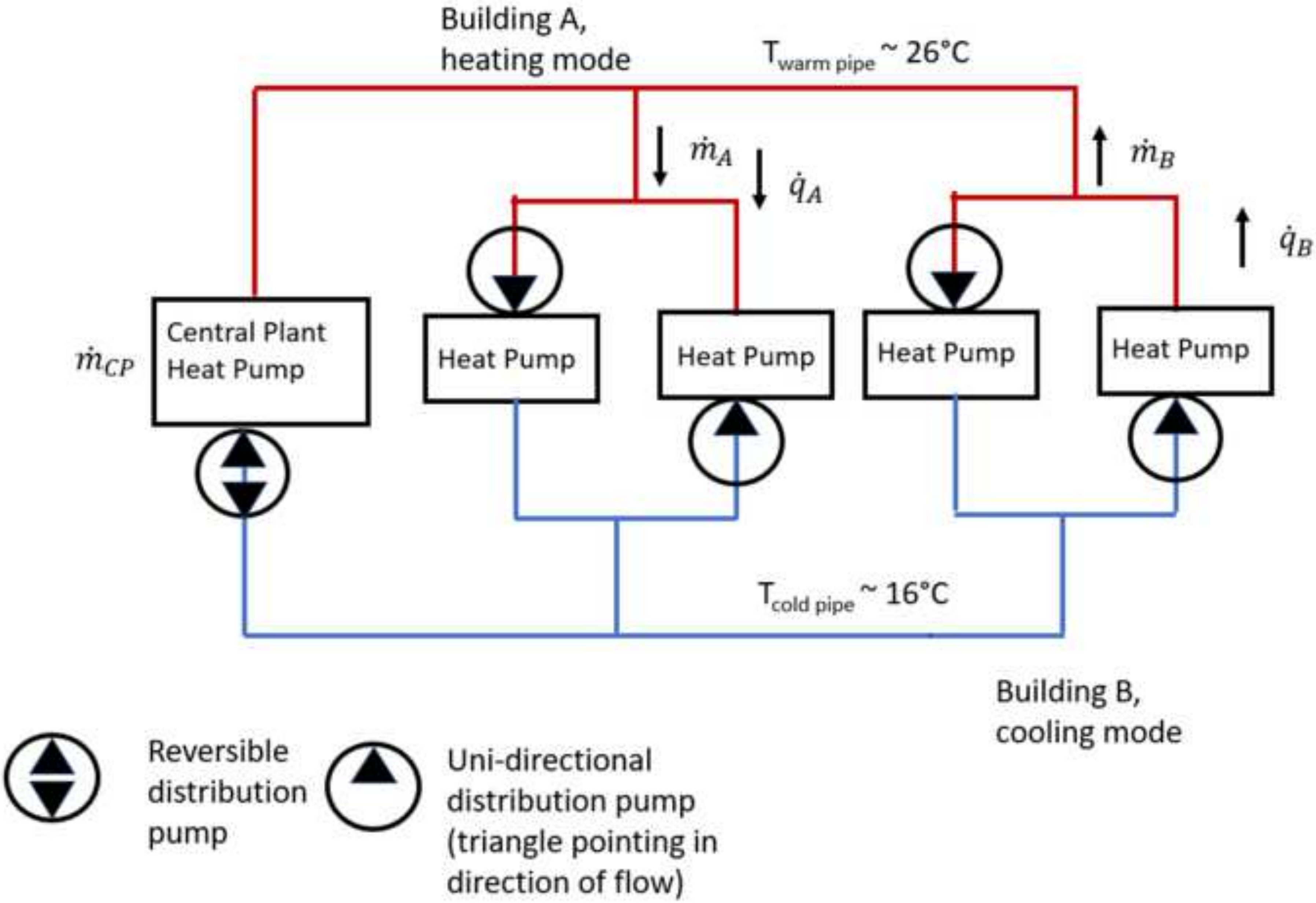
Building A,
heading mode
$T_{\text{warm pipe}}$ ~ 26°C
$\dot{m}_A$
$\dot{q}_A$
$\dot{m}_B$
$\dot{q}_B$
$\dot{m}_{CP}$
Central Plant Heat Pump
Heat Pump
Heat Pump
Heat Pump
Heat Pump
$T_{\text{cold pipe}}$ ~ 16°C
Building B,
cooling mode
Reversible distribution pump
Uni-directional distribution pump (triangle pointing in direction of flow)

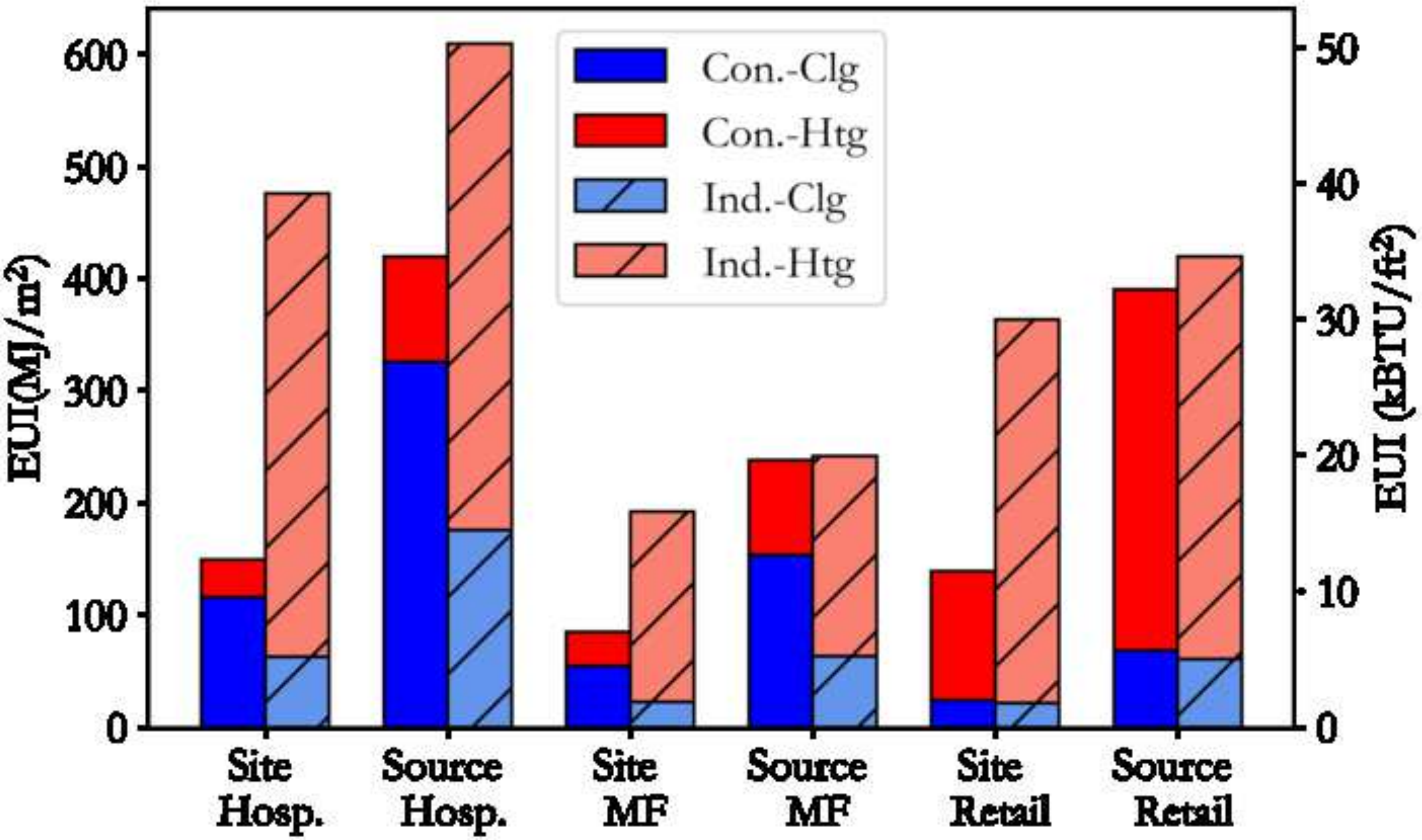
Con.-Clg
Con.-Htg
Ind.-Clg
Ind.-Htg
EUI(MJ/m^2)
EUI (kBTU/ft^2)
0
100
200
300
400
500
600
0
10
20
30
40
50
Site Hosp.
Source Hosp.
Site MF
Source MF
Site Retail
Source Retail

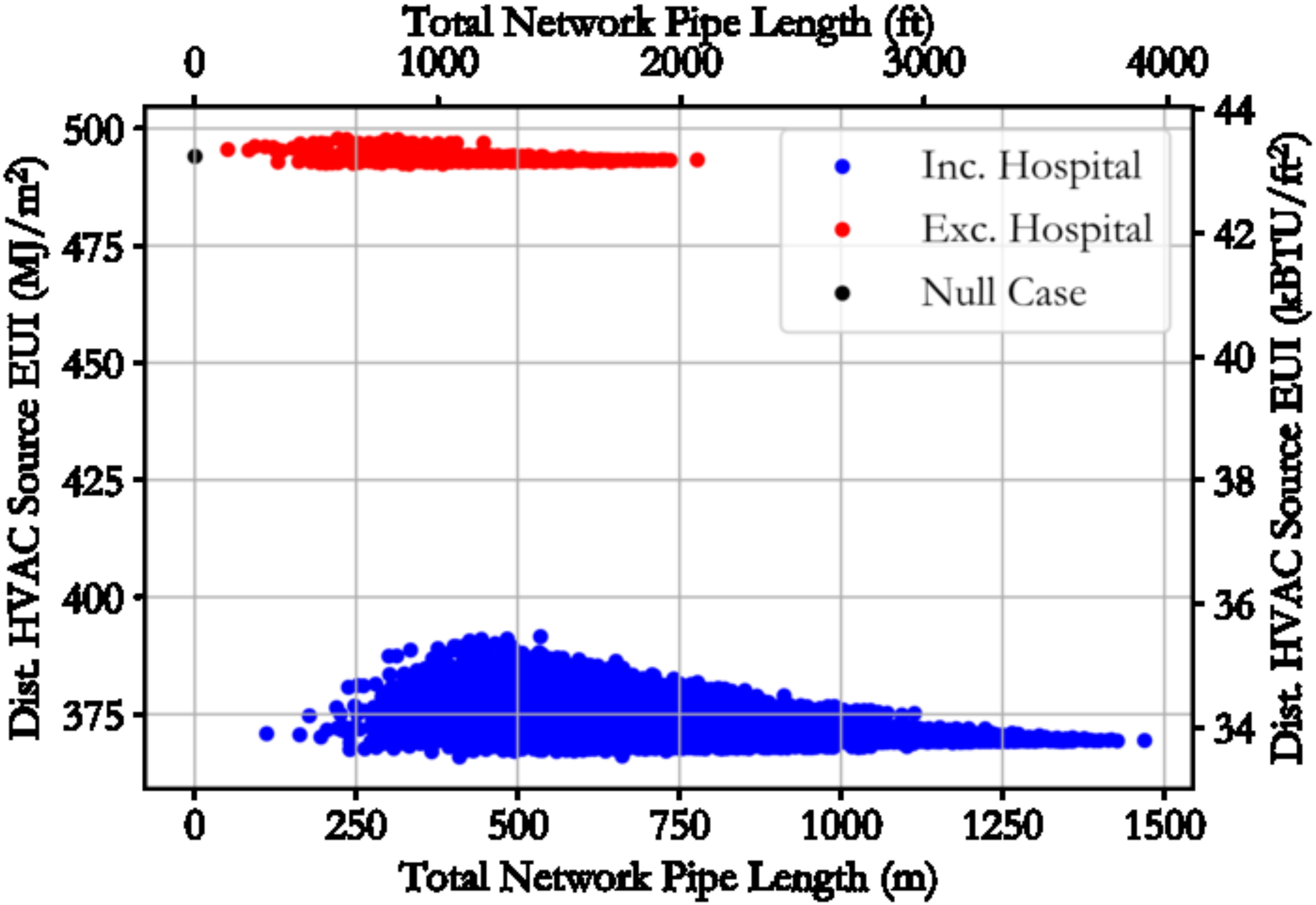
Total Network Pipe Length (ft)
0
1000
2000
3000
4000
Dist. HVAC Source EUI (MJ/m^2)
500
475
450
425
400
375
Dist. HVAC Source EUI (kBTU/ft^2)
44
42
40
38
36
34
● Inc. Hospital
● Exc. Hospital
● Null Case
0
250
500
750
1000
1250
1500
Total Network Pipe Length (m)

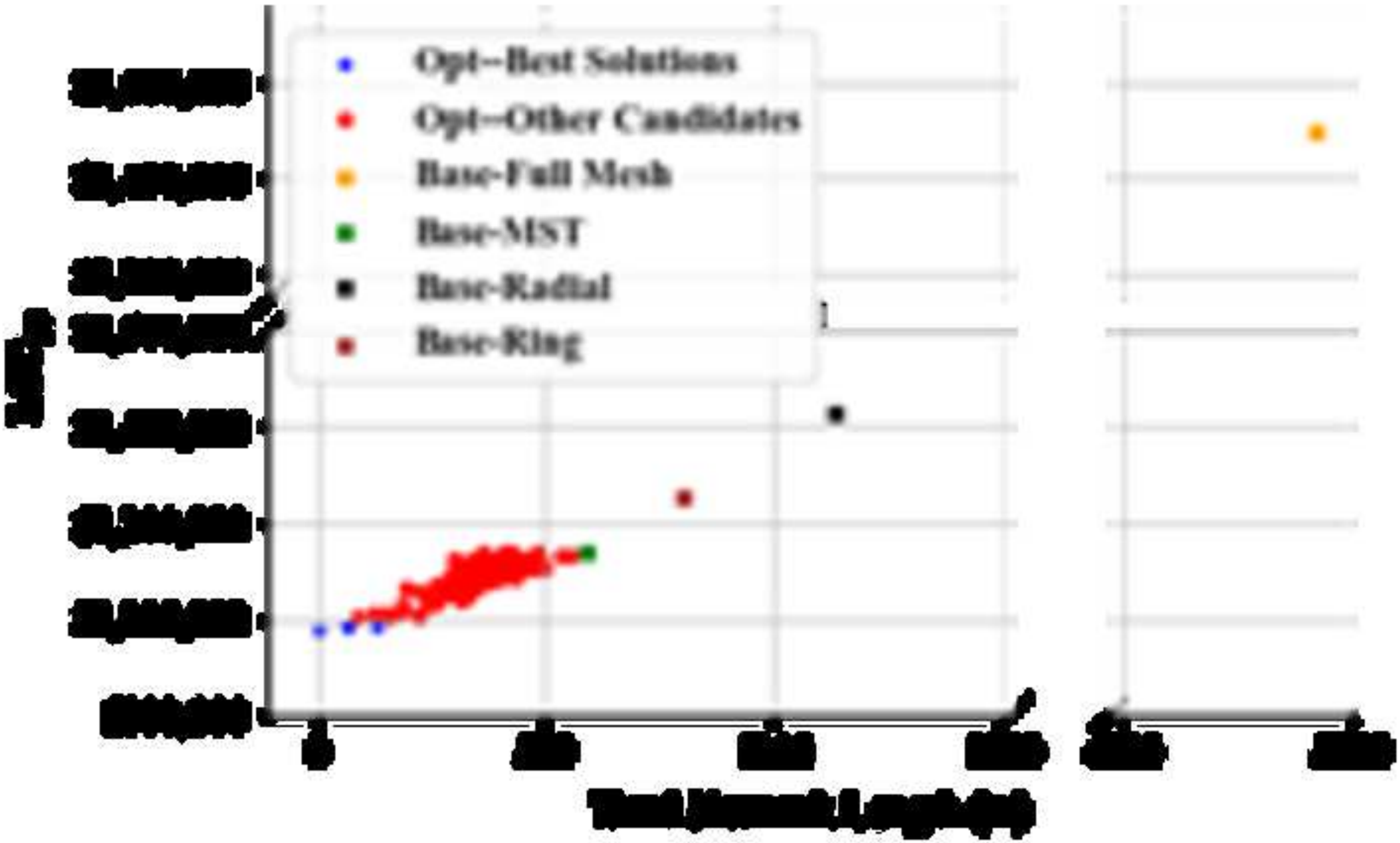
Opt--Best Solutions
Opt--Other Candidates
Base-Full Mesh
Base-MST
Base-Radial
Base-Ring

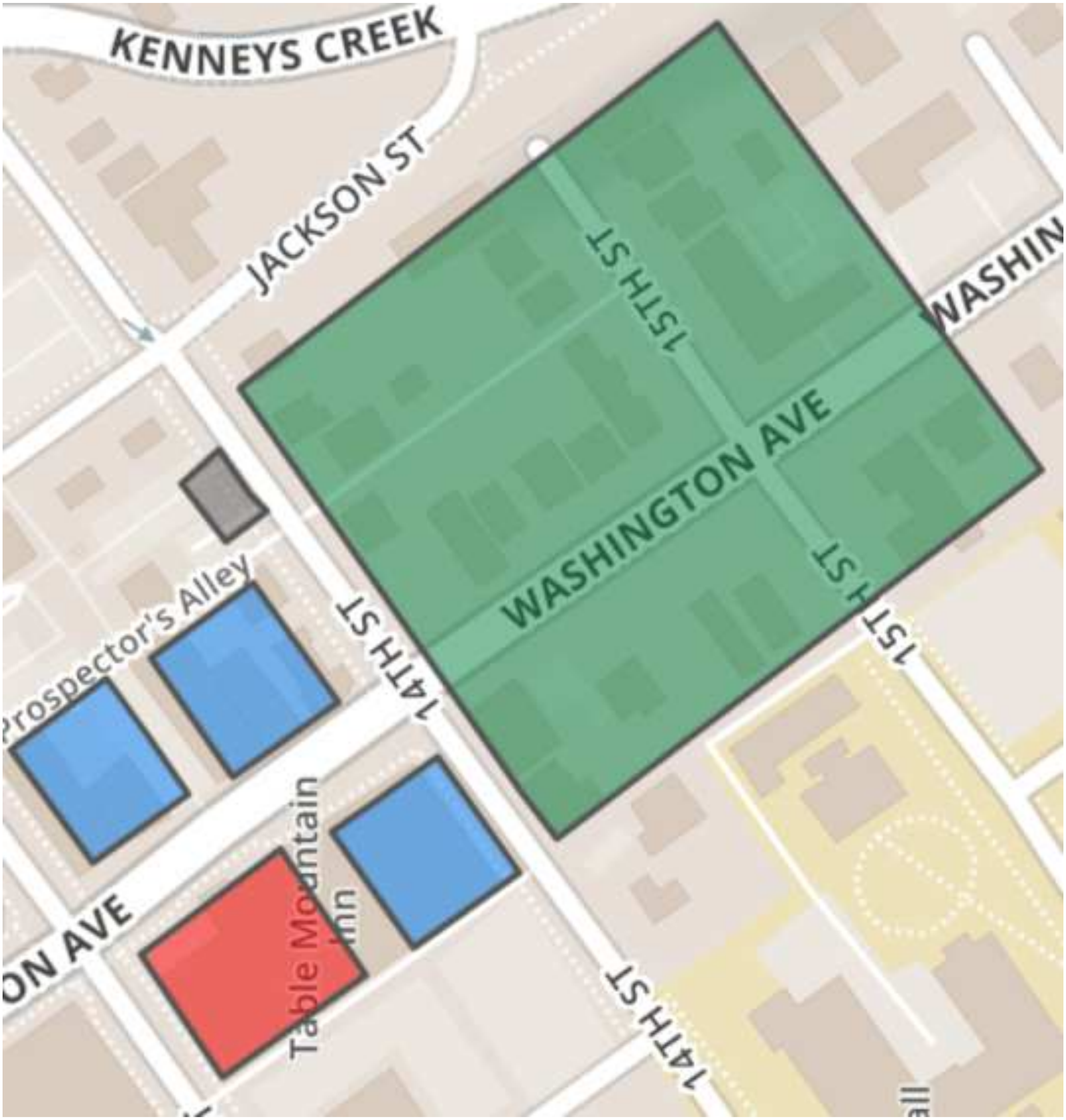
KENNEYS CREEK
JACKSON ST
15TH ST
WASHIN
WASHINGTON AVE
15TH ST
15T
Prospector's Alley
14TH ST
Table Mountain Inn
ON AVE
14TH ST

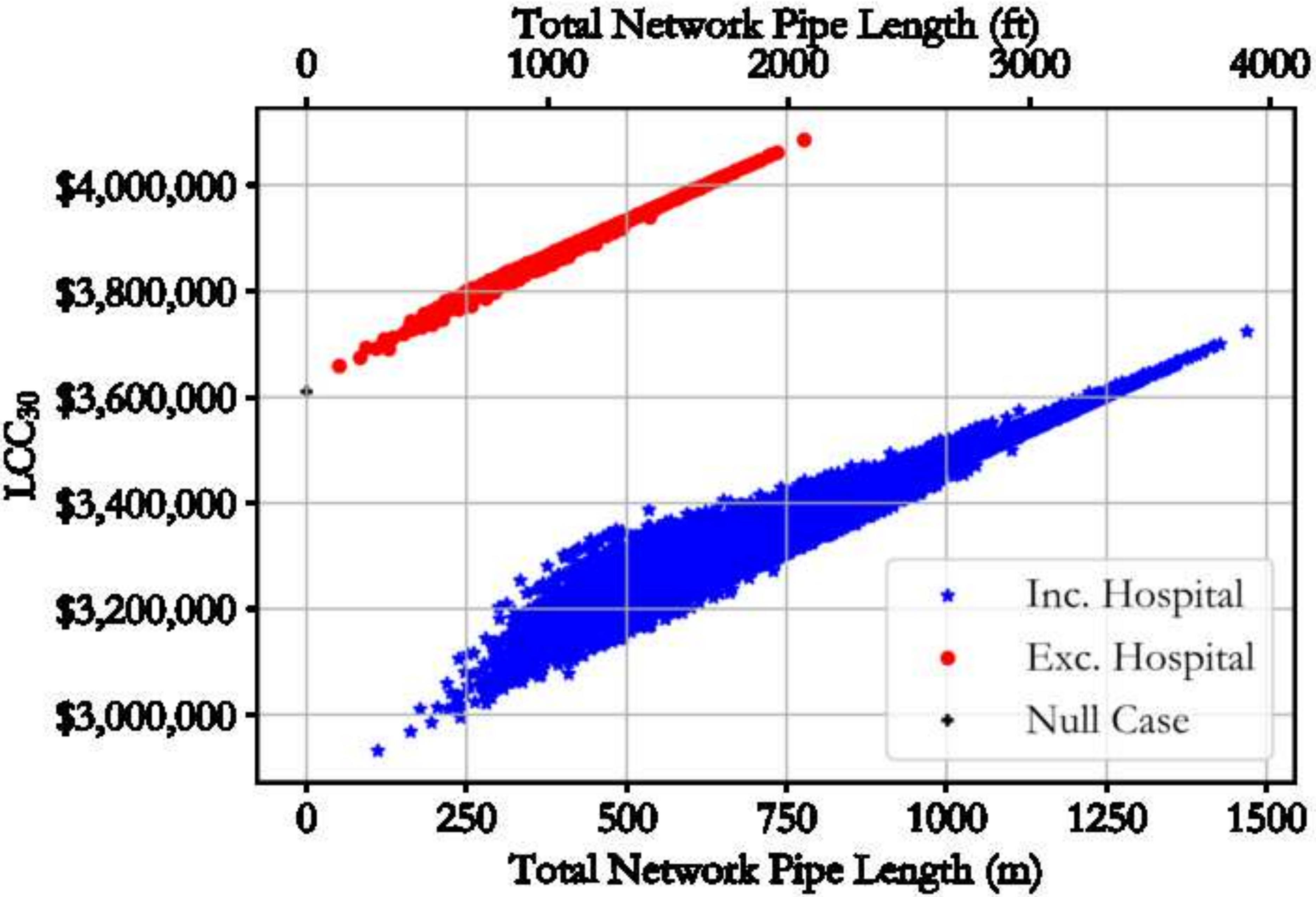
Total Network Pipe Length (ft)
0
1000
2000
3000
4000
$4,000,000
$3,800,000
$3,600,000
$3,400,000
$3,200,000
$3,000,000
LCC30
Inc. Hospital
Exc. Hospital
Null Case
0
250
500
750
1000
1250
1500
Total Network Pipe Length (m)

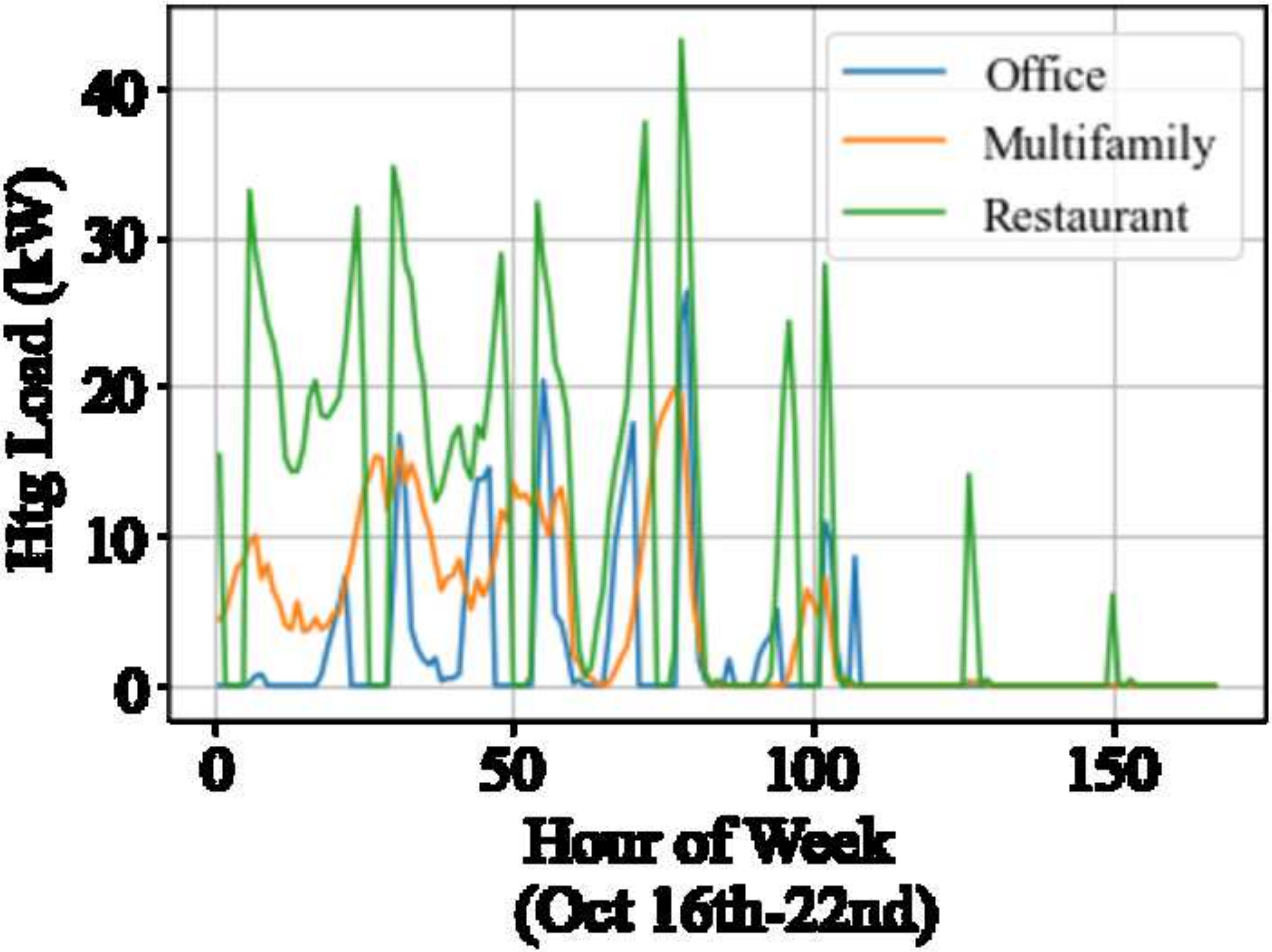
Office
Multifamily
Restaurant
Htg Load (kW)
0
10
20
30
40
0
50
100
150
Hour of Week
(Oct 16th-22nd)

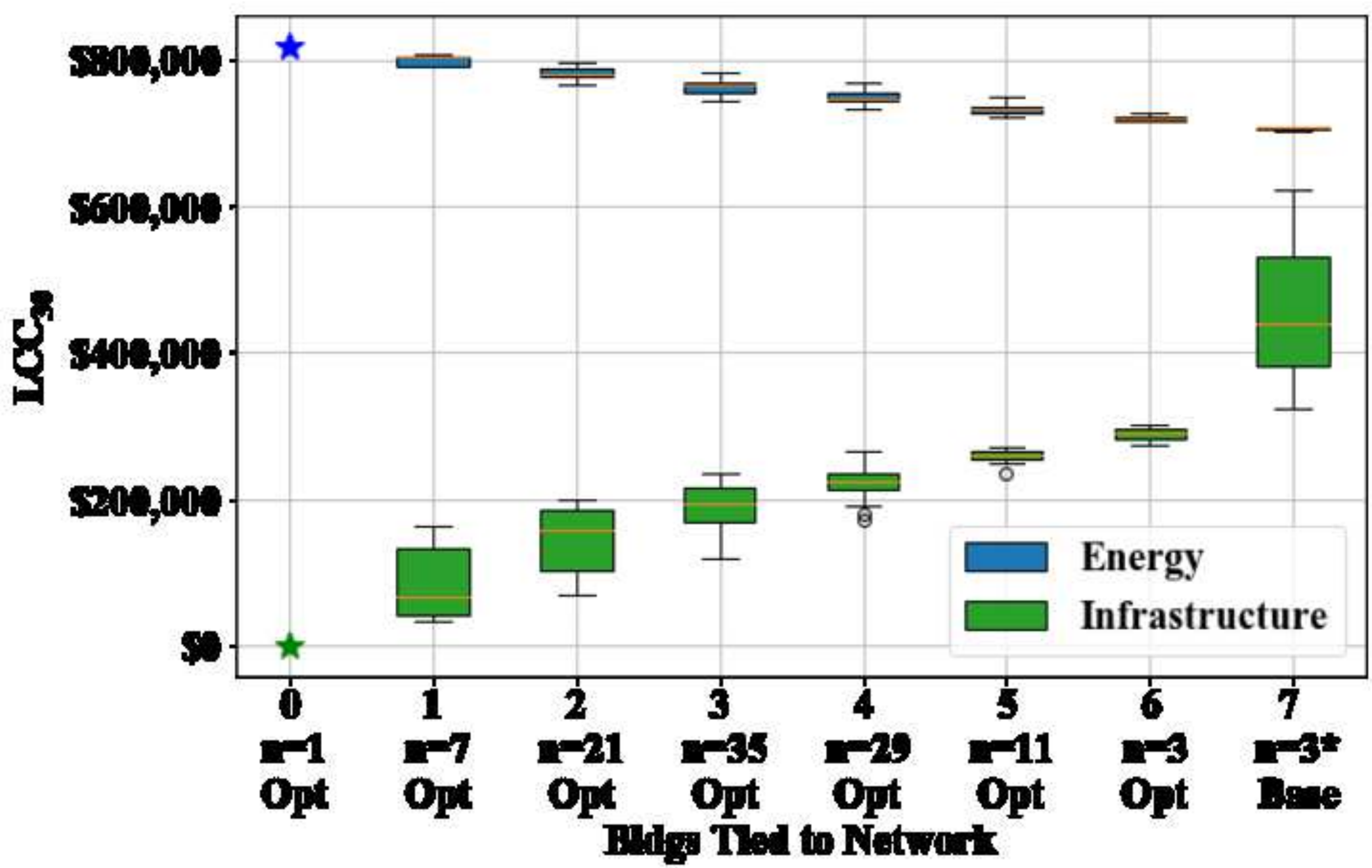
$800,000
$600,000
$400,000
$200,000
$0
LCC30
Energy
Infrastructure
0 n=1 Opt
1 n=7 Opt
2 n=21 Opt
3 n=35 Opt
4 n=29 Opt
5 n=11 Opt
6 n=3 Opt
7 n=3* Base
Bldgs Tied to Network

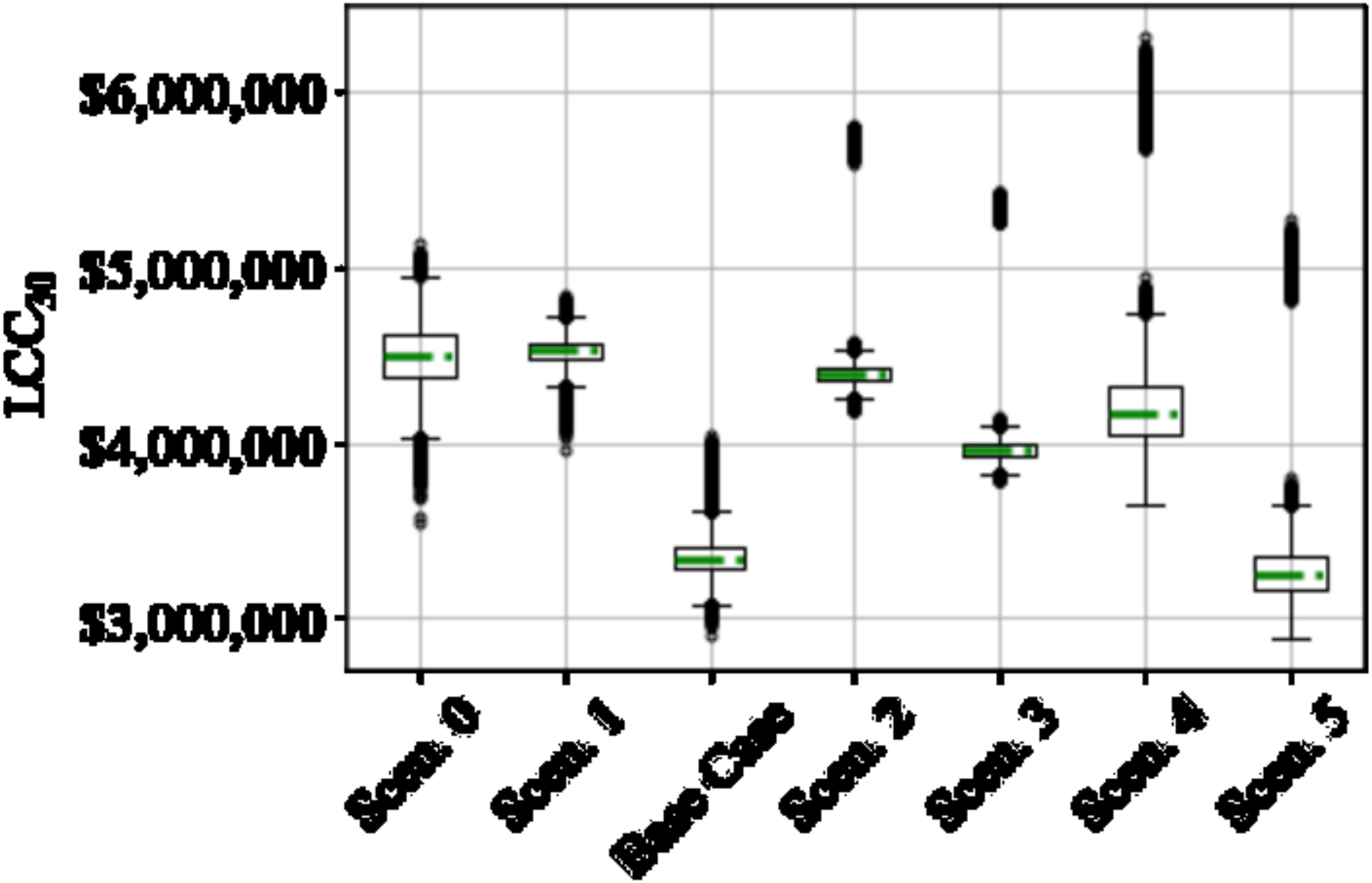

$6,000,000
$5,000,000
$4,000,000
$3,000,000
LCC_{30}
Scen. 0
Scen. 1
Base Case
Scen. 2
Scen. 3
Scen. 4
Scen. 5

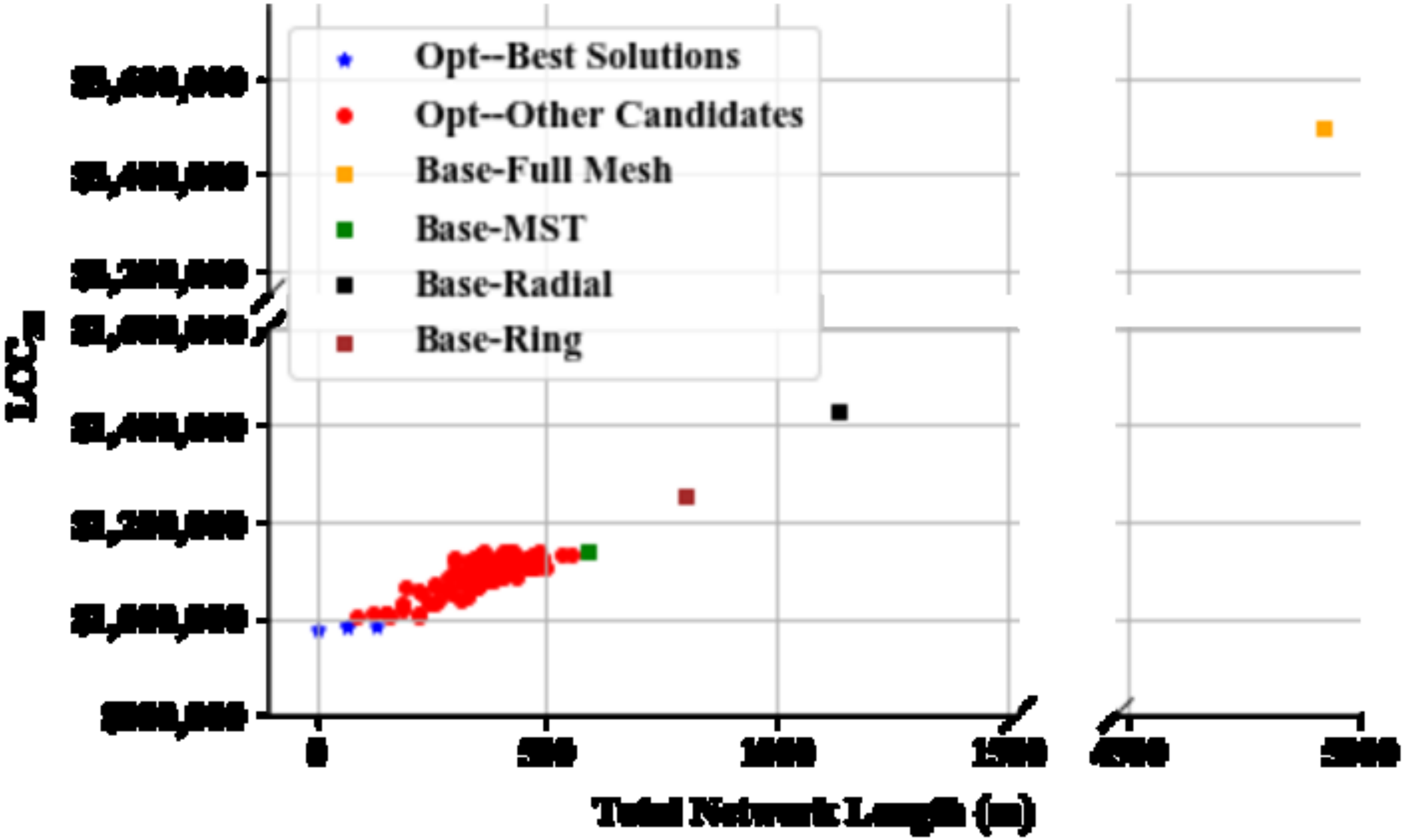
★ Opt--Best Solutions
● Opt--Other Candidates
■ Base-Full Mesh
■ Base-MST
■ Base-Radial
■ Base-Ring
$3,600,000
$3,400,000
$3,200,000
$1,600,000
$1,400,000
$1,200,000
$1,000,000
$800,000
LCC
0
500
1000
1500
4500
5000
Total Network Length (m)

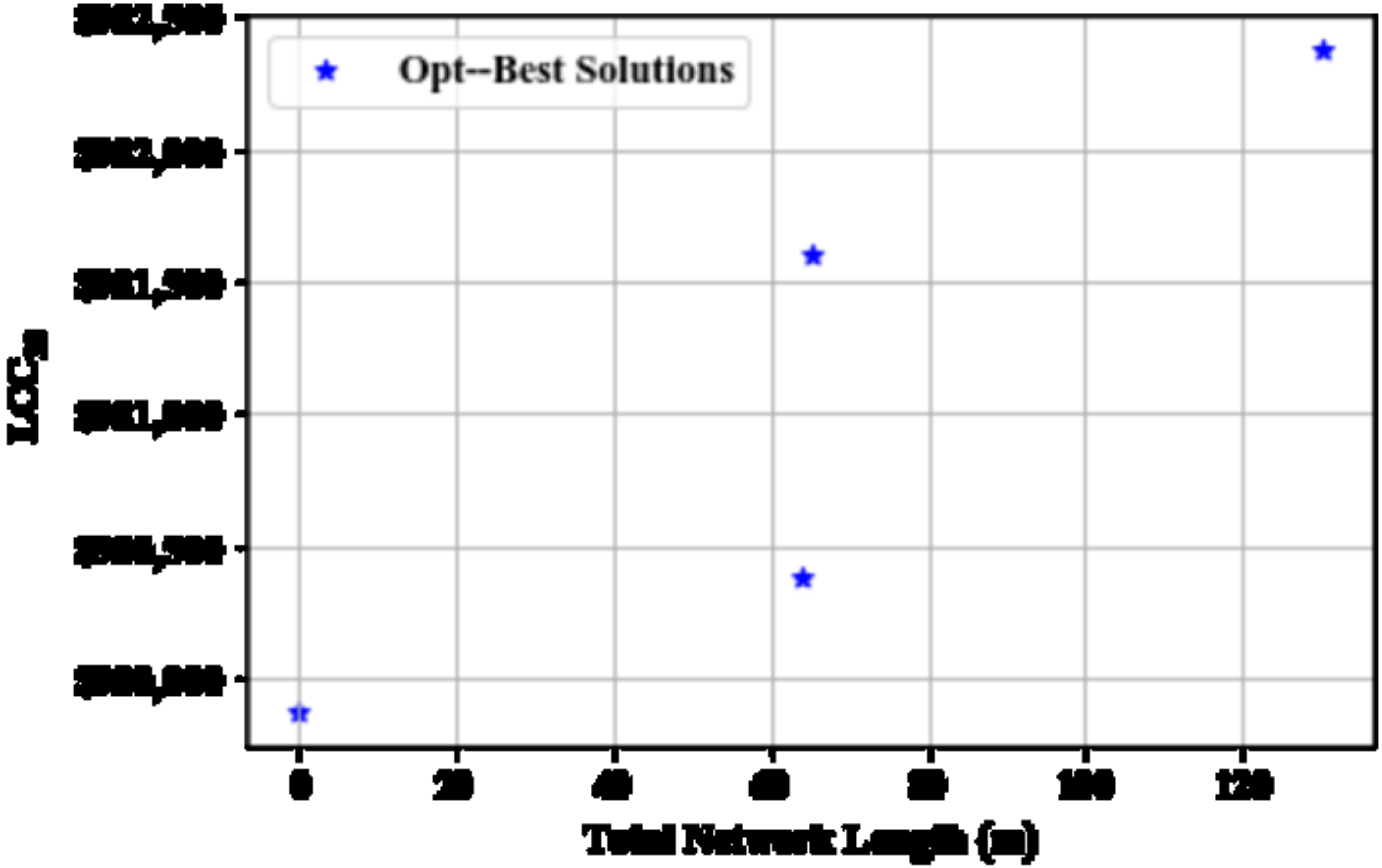
★ Opt--Best Solutions
LCC
0
20
40
60
80
100
120
Total Network Length (m)

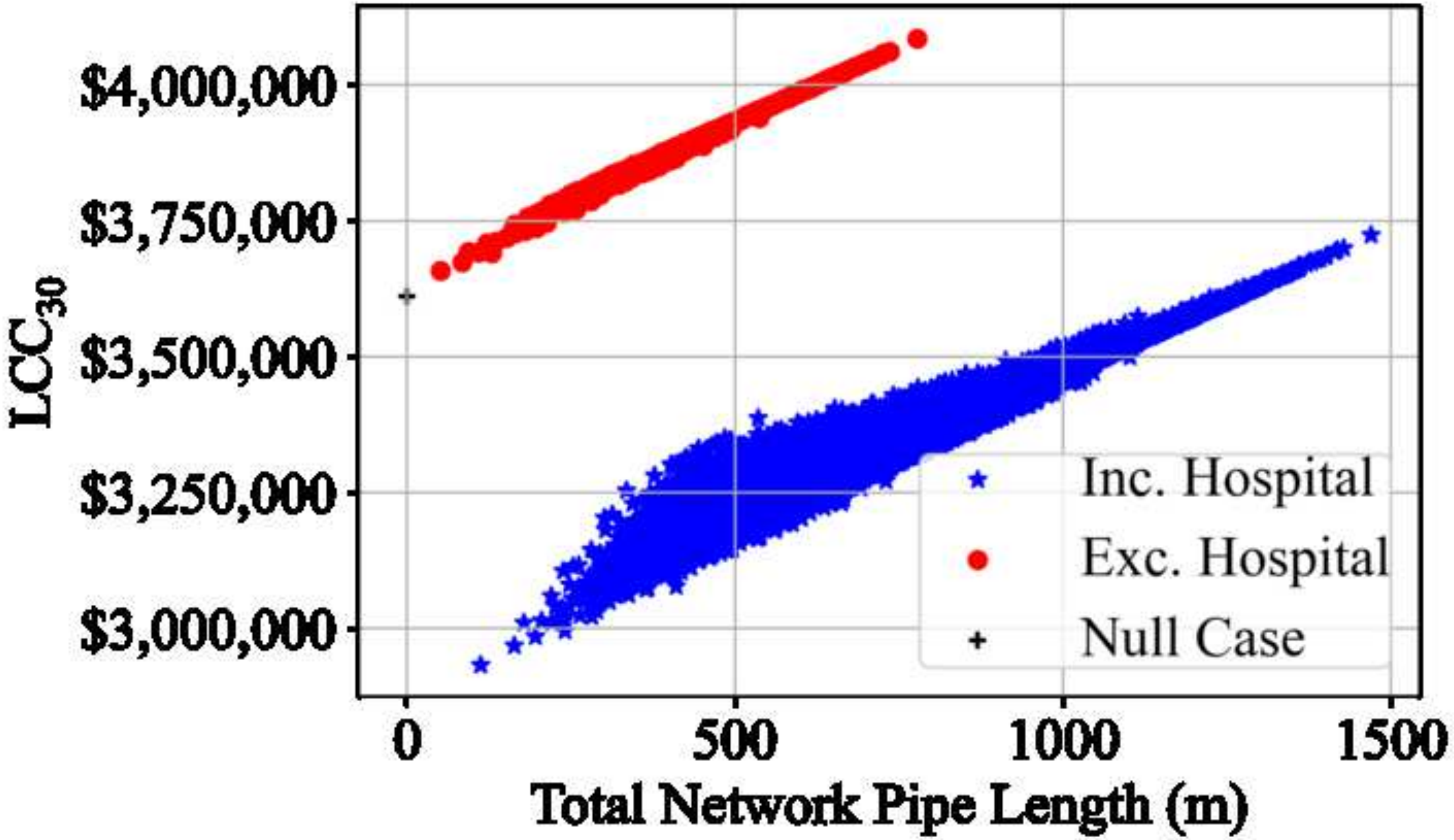
$4,000,000
$3,750,000
$3,500,000
$3,250,000
$3,000,000
LCC30
0
500
1000
1500
Total Network Pipe Length (m)
Inc. Hospital
Exc. Hospital
Null Case

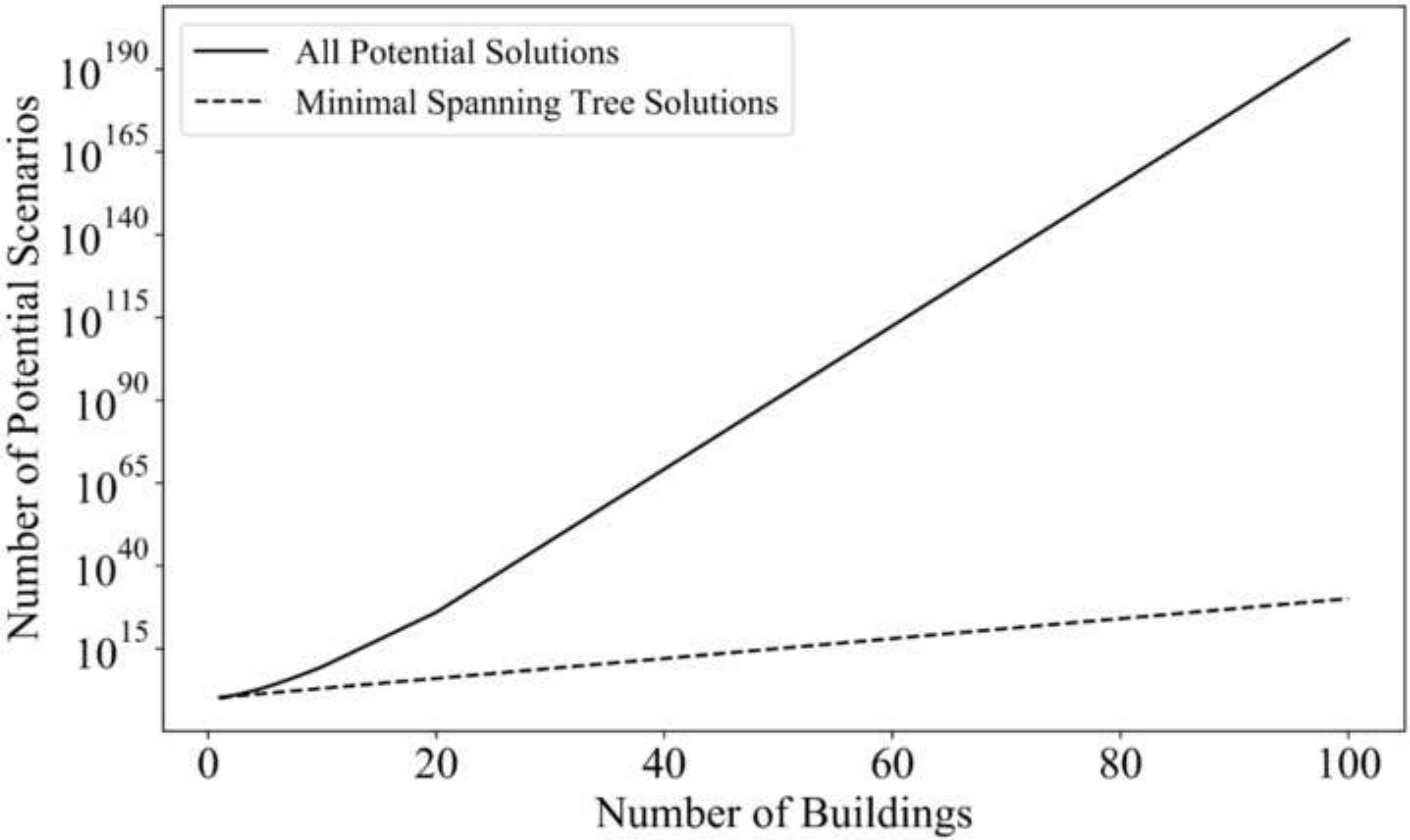
All Potential Solutions
Minimal Spanning Tree Solutions
Number of Potential Scenarios
10^{190}
10^{165}
10^{140}
10^{115}
10^{90}
10^{65}
10^{40}
10^{15}
0
20
40
60
80
100
Number of Buildings

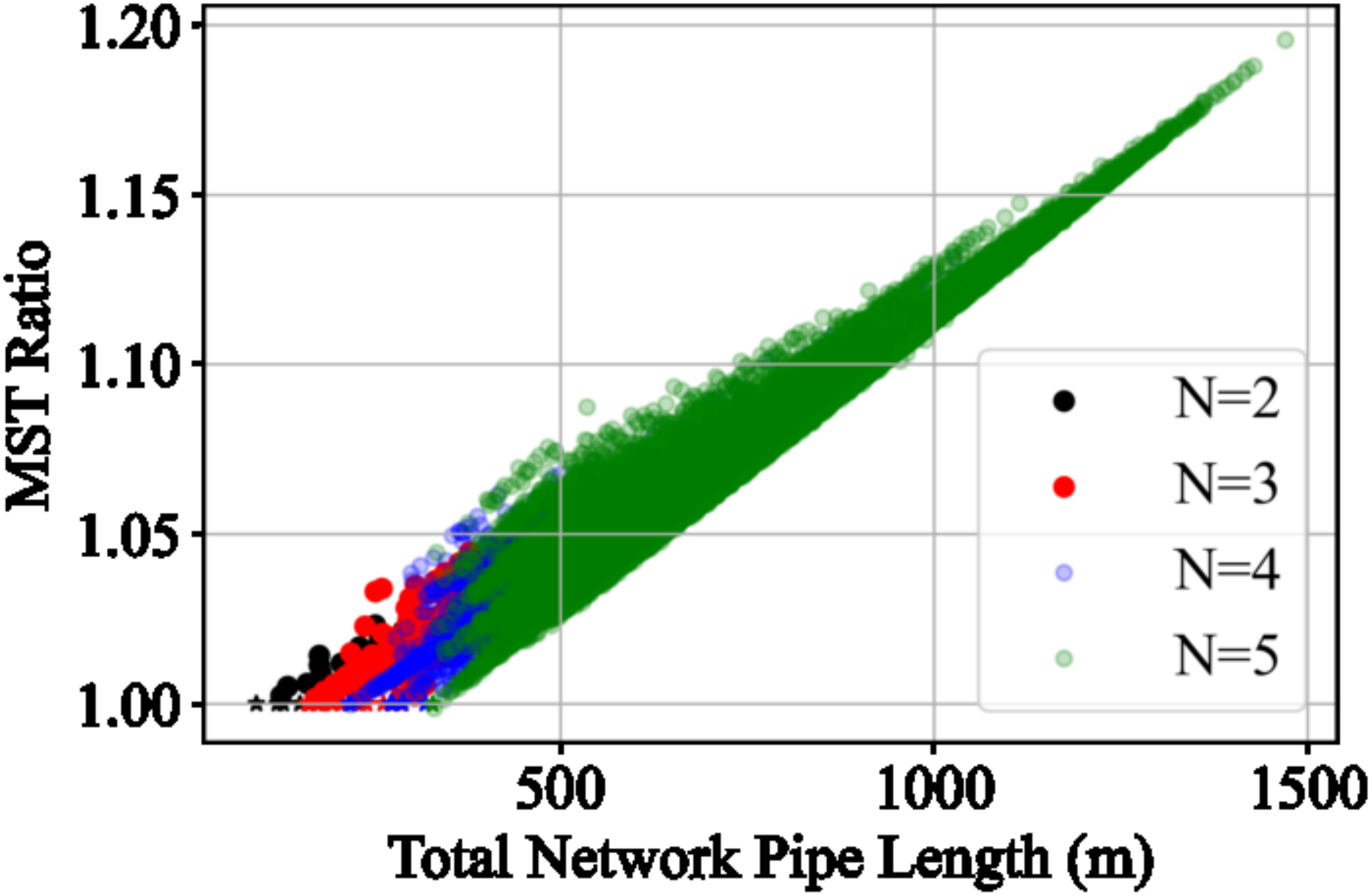
1.20
1.15
1.10
1.05
1.00
MST Ratio
500
1000
1500
Total Network Pipe Length (m)
N=2
N=3
N=4
N=5

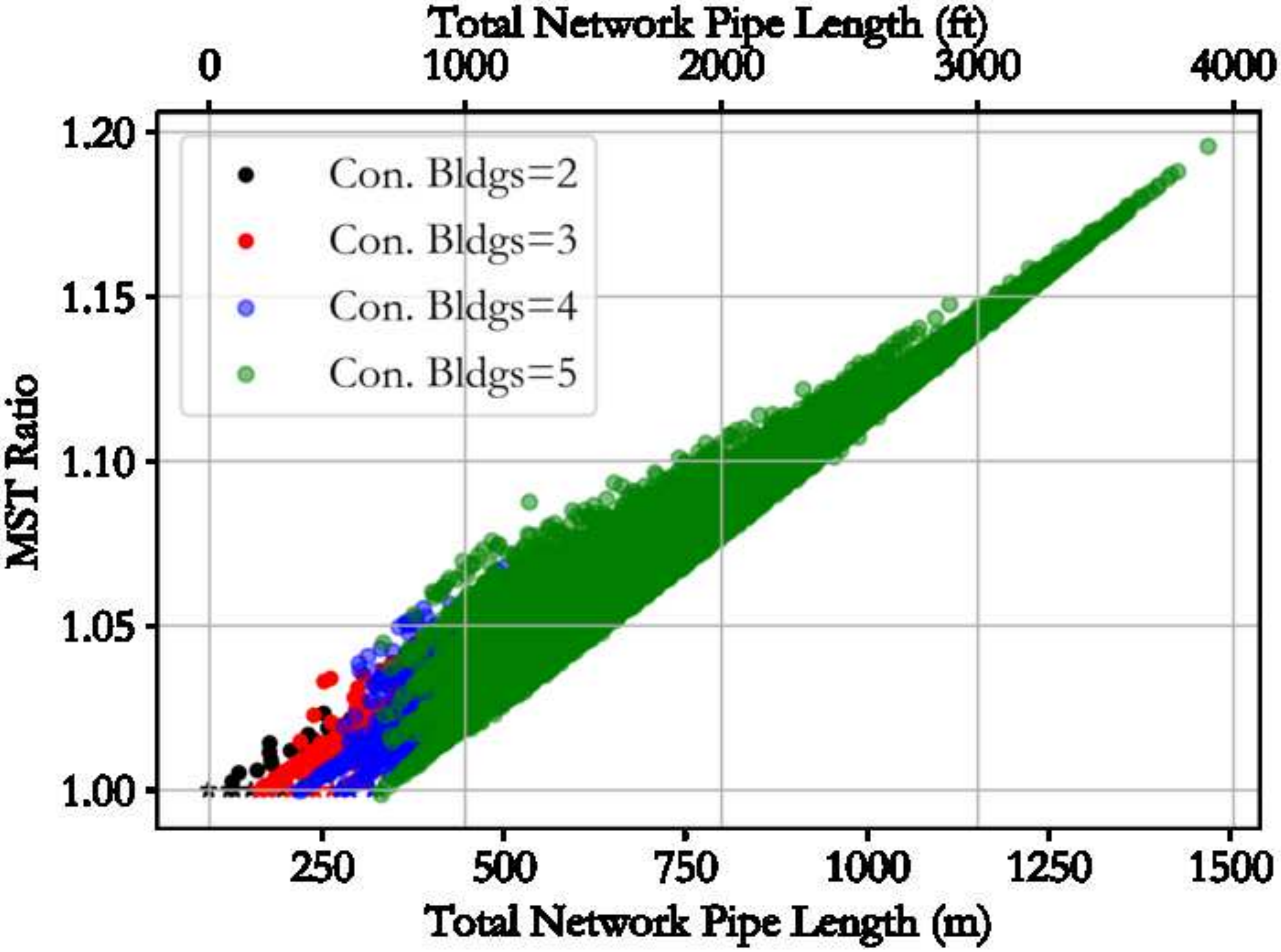
Total Network Pipe Length (ft)
0
1000
2000
3000
4000
MST Ratio
1.20
1.15
1.10
1.05
1.00
● Con. Bldgs=2
● Con. Bldgs=3
● Con. Bldgs=4
● Con. Bldgs=5
250
500
750
1000
1250
1500
Total Network Pipe Length (m)

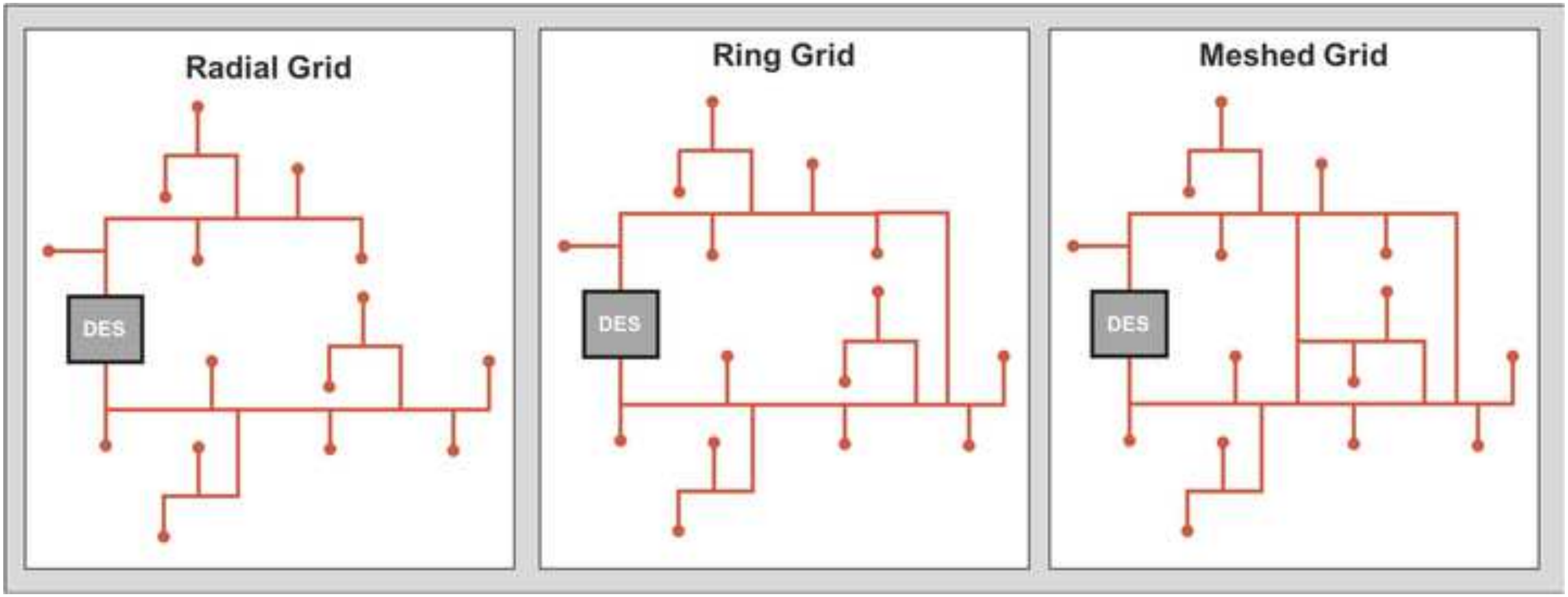
Radial Grid
DES
Ring Grid
DES
Meshed Grid
DES

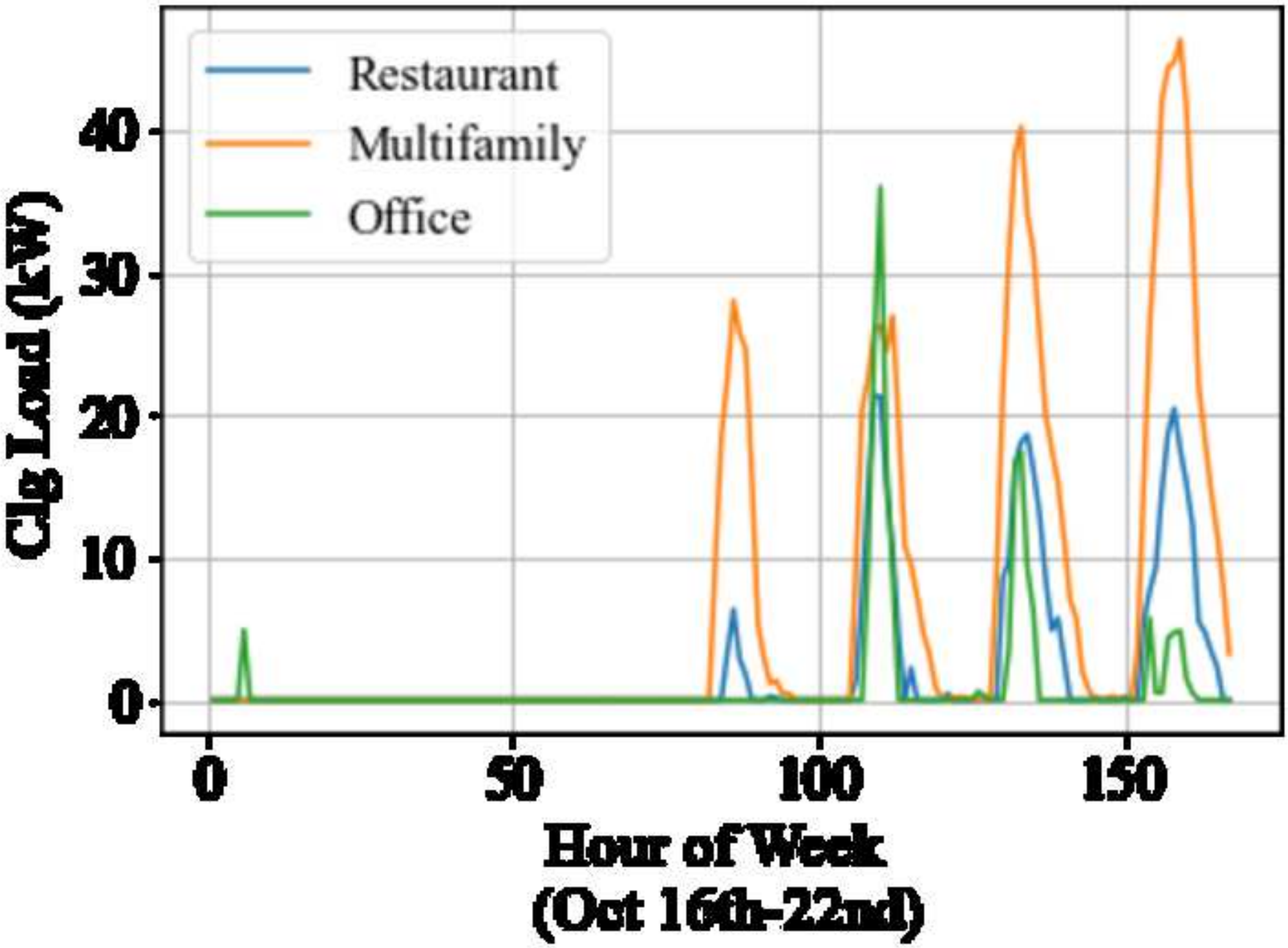
Restaurant
Multifamily
Office
Clg Load (kW)
0
10
20
30
40
0
50
100
150
Hour of Week
(Oct 16th-22nd)

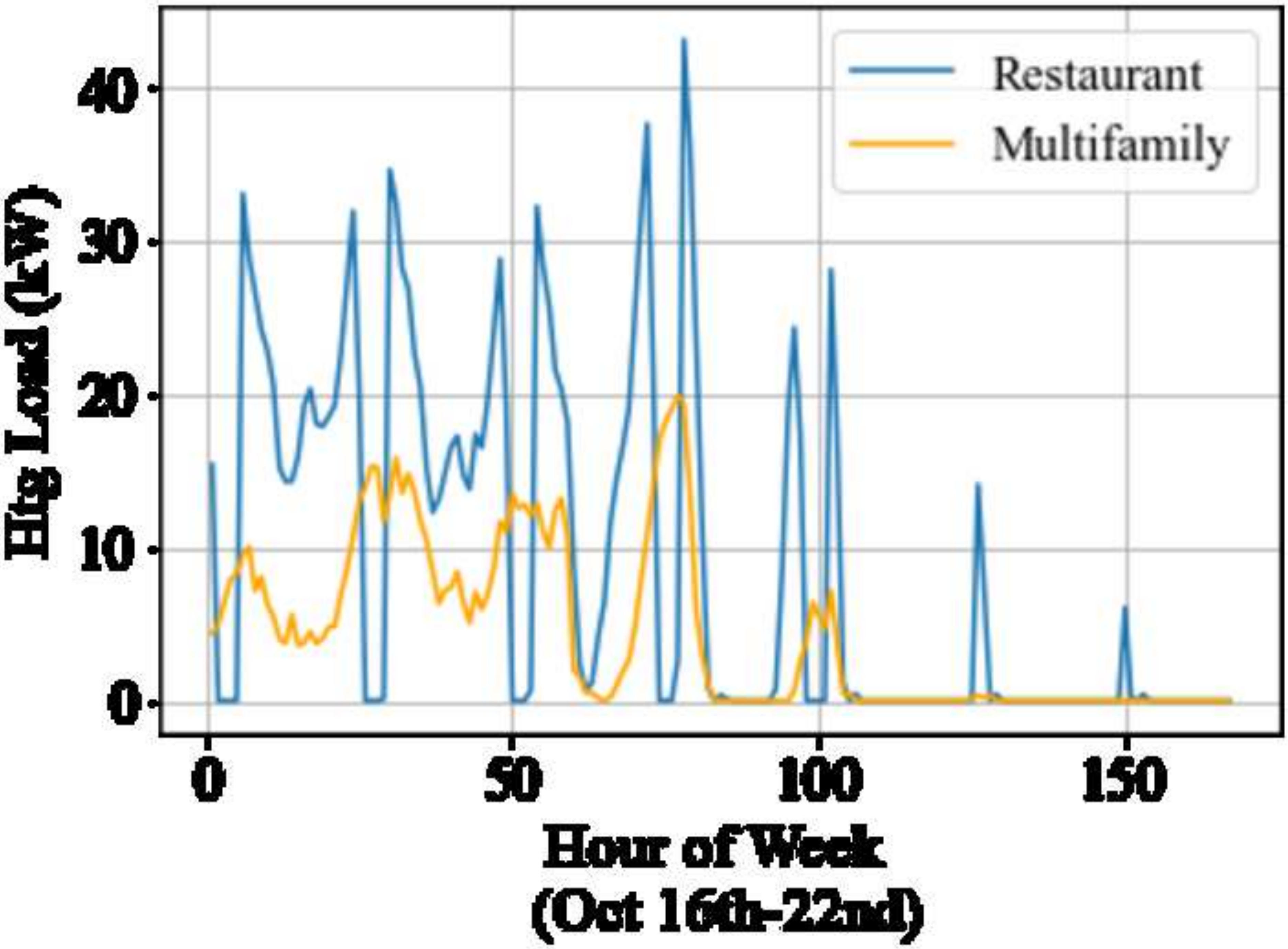
Restaurant
Multifamily
Htg Load (kW)
0
10
20
30
40
0
50
100
150
Hour of Week
(Oct 16th-22nd)

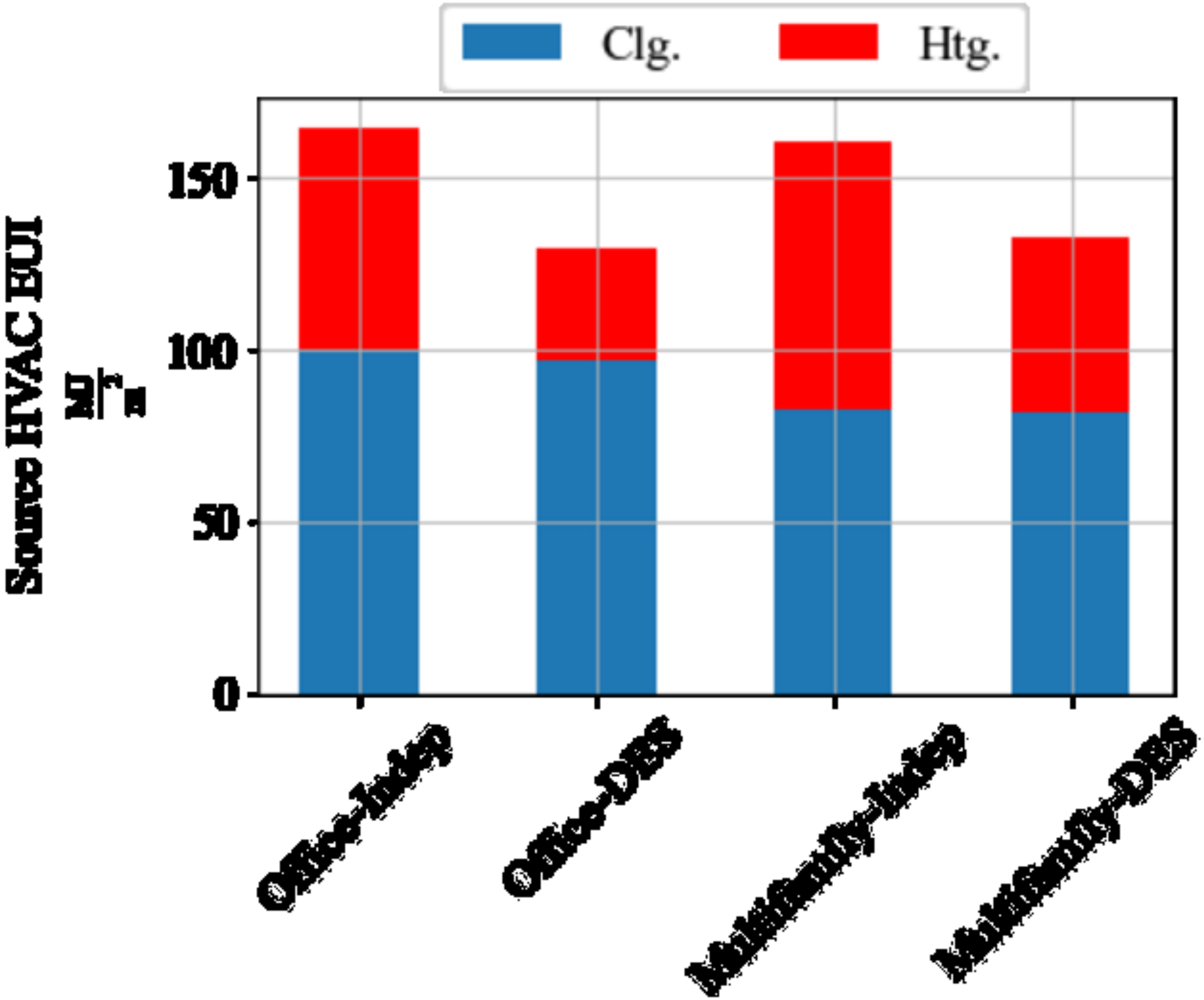
Clg.
Htg.
Source HVAC EUI
$\frac{MJ}{m^2}$
0
50
100
150
Office-Indep
Office-DES
Multifamily-Indep
Multifamily-DES

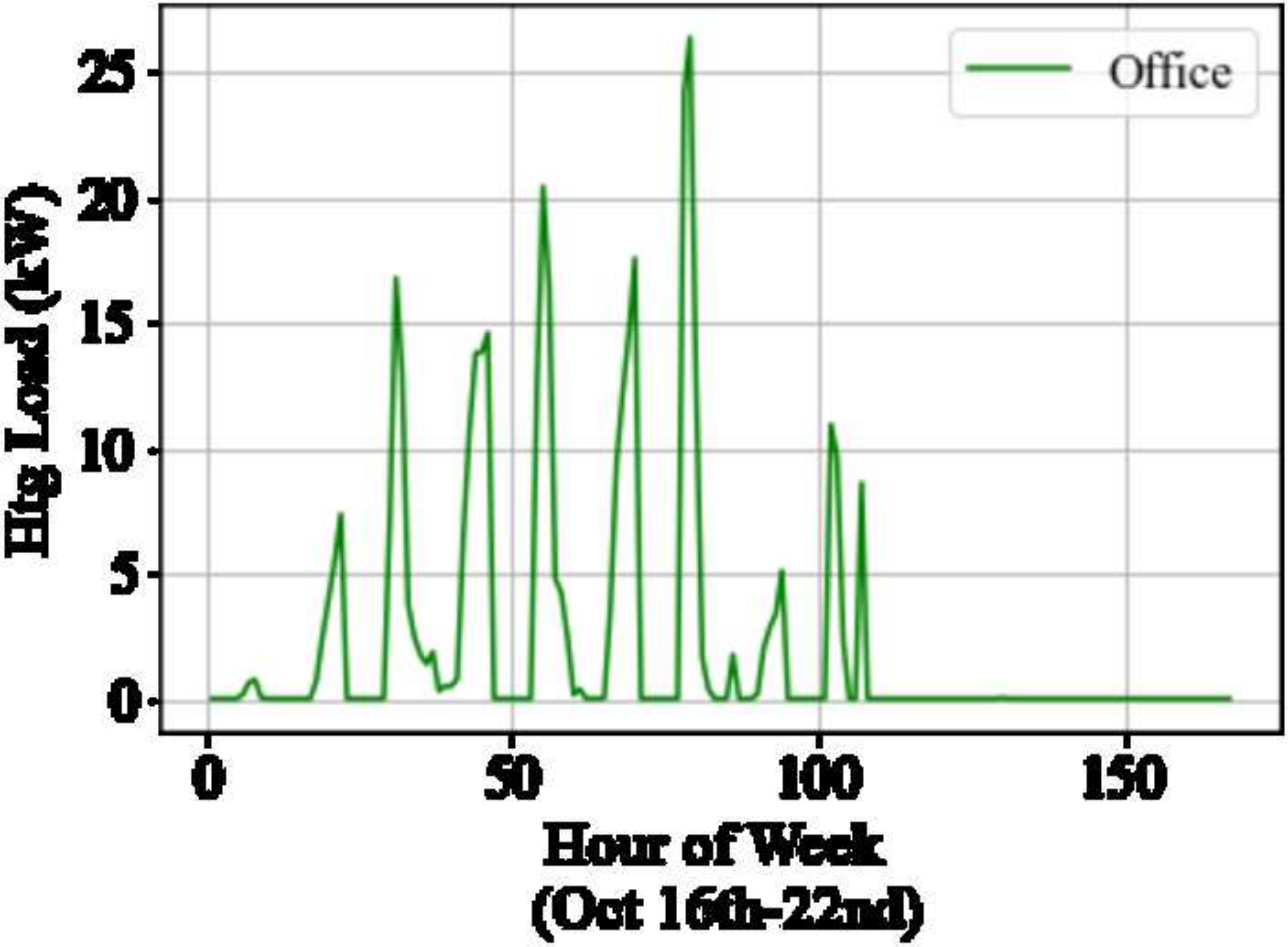
Office
Htg Load (kW)
0
5
10
15
20
25
0
50
100
150
Hour of Week
(Oct 16th-22nd)

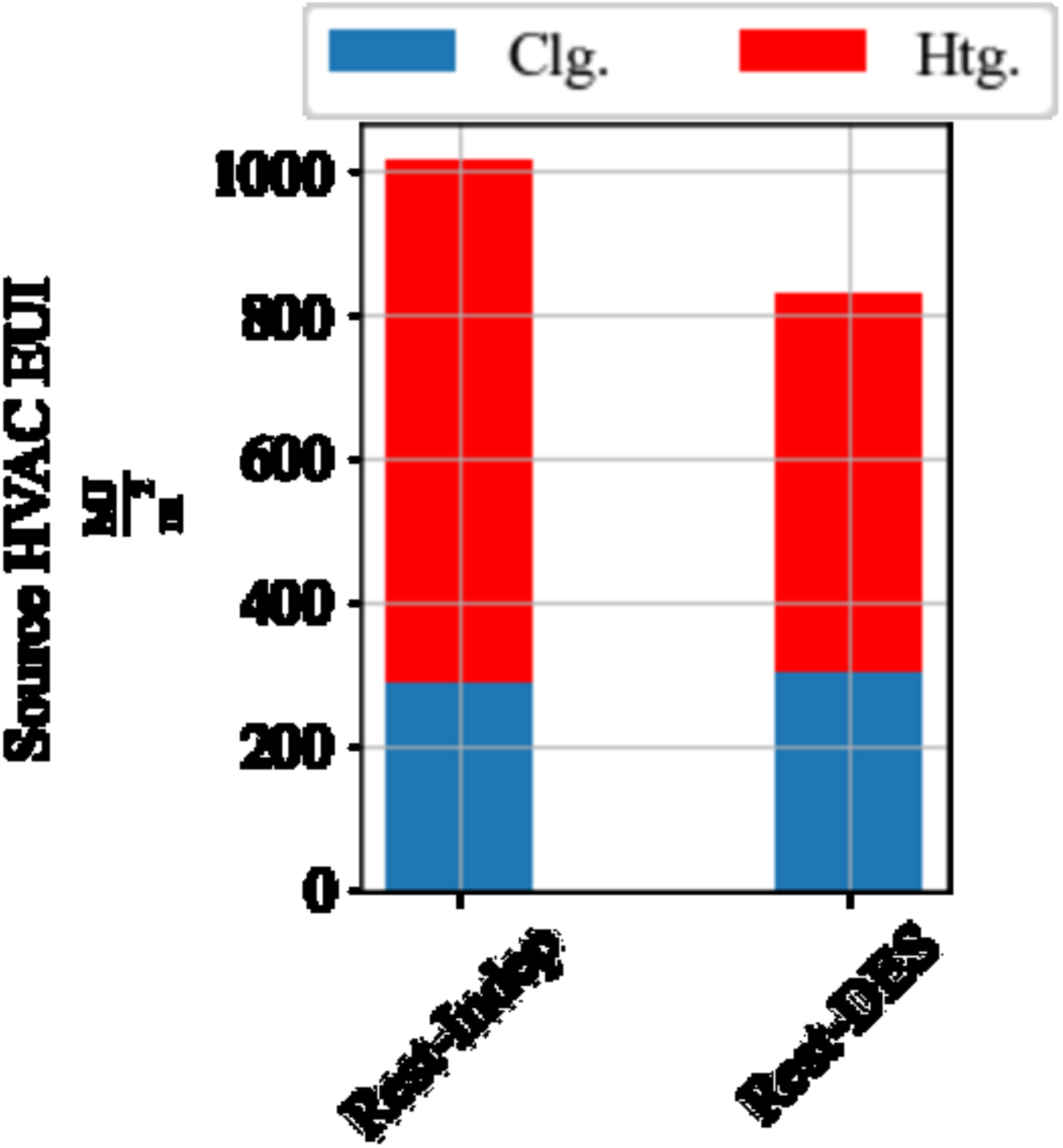
Clg.
Htg.
Source HVAC EUI
$\frac{MJ}{m^2}$
1000
800
600
400
200
0
Rest-Indep.
Rest-DES

Credit Author Statement

Amy Allen: Writing- Original draft preparation, conceptualization, formal analysis. Gregor Henze: Conceptualization, writing - review & editing. Kyri Baker: Conceptualization, writing - review & editing. Gregory Pavlak: Conceptualization, writing - review & editing. Michael Murphy: Conceptualization, writing - review & editing, formal analysis.

Declaration of Interest Statement

Declaration of interests

☒ The authors declare that they have no known competing financial interests or personal relationships that could have appeared to influence the work reported in this paper.

☐The authors declare the following financial interests/personal relationships which may be considered as potential competing interests:

(I have signed on behalf of all authors—Amy Allen.)